

Conceptual Design of an Autonomous Asteroid Mining Robot

Research Internship Project Report

Society for
Space
Education
Research &
Development



Project Guide: **Ms. Rashika SN**

Internship and Projects Division (IPD),
Society for Space Education Research and Development (SSERD)

Team Vulcans
September, 2020

To Our Family, Teachers and Friends

Acknowledgement

A very special thanks to **Ms. Rashika SN**, our Project Guide for her valuable contribution in narrowing down our research to the most crucial points essential for Space Missions. She shared with us important references and guidelines to follow and helped us conceptualize a Real Space Mining Mission. She monitored our work all the way throughout and gave valuable suggestions and feedback.

We extend our gratitude to **Mr. Mahesh**, our Internal Mentor for always guiding us in our research by critically evaluating our work and suggesting ideas and improvements.

By the end of this internship, we were able to explore challenges and opportunities that accompany Research, more importantly Space Research. We have developed a fresh passion in our interests in our respective fields. Strict deadlines bestowed upon the sense of responsibility, **Weekly Presentations** and **Team Meetings** helped us develop better communication skills, **Training sessions** and **Tech Talks** contributed significantly to our knowledge and perspective. This research helped us recognize our hidden potential in brainstorming ideas and shaping them to fit the purpose. All this learning in just 5 weeks, would not have been made possible if not for the SSERD Team. A very big thanks to the **Society for Space Education Research and Development** for this wonderful initiative and Internship opportunity.

The Team

Atreya G Bhat
Kashyap Hegade K S
Ankith D H
Jayaprakash B Shivakumar
Marcelo Fernando Condori Mendoza
Aayush Rawat
Dipti Lode
AVN Ravi
Mehul Srivastava
Sumanth Nethi
Madhavi Swamy
Izza
Yaseer Meera
Bharat Bhavsar

Abstract

Water, one of the most important building blocks of Life is present in large amounts on asteroids which can be used as rocket fuel, as life support for astronauts and also as Radiation shield. As such, water can be the key for **Human Deep Space Exploration** and potentially setting up **Human Space Colonies**. The Earth cannot be exploited anymore and one of the solutions is mining potential Near Earth Asteroids which contain valuable metals and minerals. While bringing back valuable metals like gold and platinum from asteroids to Earth and selling them at high prices seems a natural choice, we can do more than that. In this report, we present the concept of an **Asteroid Mining Robot** to extract water from C-type asteroids, autonomously. The prospect asteroid selected for our mission is **(341843) 2008 EV5**. The proposed Lander design involves the structure, methods of mining and different subsystems which are crucial for the mission, especially for the mining phase.

Contents

Contents	vi
1 Environmental Analysis	1
1.1 Introduction	1
1.2 Asteroid Prospection	2
1.2.1 Important Factors	2
1.2.2 Purpose of Targeting C-Type Asteroids	2
1.2.3 Narrowing Down to Particular Asteroids	3
1.2.4 A Comparative Study	3
1.3 Conclusion	6
1.3.1 2008 EV5	6
1.4 Challenges	7
2 Design Overview	8
2.1 Brief Description of the Proposed Lander Design	8
2.2 Anchoring to the Asteroid: Microspine Anchoring Technology	8
2.2.1 Introduction	8
2.2.2 Gripper Construction and Working principle	10
2.2.3 Experimental Results	11
2.3 Drilling Assembly and Mobility Intuition	12
3 Drilling and Extraction	15
3.1 Drilling Technique	15
3.2 Heating the soil	16
3.2.1 Challenges	16

3.2.2	Technique Proposed	17
3.2.3	Results	17
4	Sensors and cameras	20
4.1	Main Structure Design	20
4.2	Proposal for Implementation of Sensors and other Electronic Modules . .	21
4.2.1	Space Robotics LIDAR System	21
4.2.2	Spacecraft Positioning	22
4.2.3	Scientific Objectives and Conclusions from Laser Altimeter (LIDAR) Light Detection And Ranging	24
4.3	Optical Navigation Camera	25
4.4	Sensors used in the mining process	27
5	Power Subsystem	30
5.1	Introduction	30
5.2	Power Source Design	31
5.3	Battery Design	35
5.3.1	Trade-off between choosing Ni-MH and Li-ion battery	37
5.3.2	Battery calculation	37
5.4	Conclusion	37
6	Thermal Control System Analysis and Design	39
6.1	Environment	39
6.2	Preliminary Thermal Analysis	40
6.3	Model	40
6.4	Thermal Analysis	42
6.5	Thermal Control System	44
7	Future Scope - Water Electrolysis Propulsion	45
7.1	Introduction	45
7.2	Features	46
7.3	Advantages over other Propulsion Techniques	46
7.4	WINE - The World is not Enough	47
7.5	Conclusion	47
Appendix A		48
A.1	48
A.2	49

A.3	51
References	53

Environmental Analysis

1.1 | Introduction

The massive improvements in Technology and Resources have resulted in the advent of a new era in Space exploration, with a whole new level of challenges and opportunities. With a broader mindset and big goals such as returning to the moon for setting up Space colonies, numerous missions have scaled up to much higher levels. One such mission is - Autonomous Asteroid Mining System. Various space agencies like NASA and JAXA have tried and achieved success in either arriving at the asteroid or also potentially return Samples collected from the surface. These missions have given a broader perspective about these largely unknown small celestial bodies and has paved the way for the development of new technologies and also have attracted Space Enthusiasts around the world to think and develop ideas about mining on asteroids.

Team Vulcans with a 5-week effort present in this report the ideas and methods for mission requirement formulation in support of Autonomous Asteroid Mining System with study focussing on Mining on Asteroids. A variety of asteroids have been identified to contain volatile-bearing minerals, silicates, iron-nickel alloys from their spectral analysis and meteoric studies. Asteroids possess potential natural resources which can be put to use in space or can be brought back to earth. The team explored several aspects of potential benefits from rigorous researching and developing as well as modifying ideas to best suit our task. This report presents Team Vulcans' idealised concept for the Autonomous Asteroid Mining System.

1.2 | Asteroid Prospection

The in-depth knowledge of the surface of an asteroid and its mineral composition can be revealed only when an explorer spacecraft arrives and begins its exhaustive characterization in preparation for sampling. The chemical and mineralogical nature of the surface grains will become even clearer when the spacecraft returns samples to Earth. Until that time, however, inferences of surface properties rely on telescopic observations of the asteroid. Initially, certain factors which are very important for the prospection of an asteroid are explained below.

1.2.1 | Important Factors

- Amount of Data Available: The information we have about small celestial bodies like asteroids is very limited, due to their very small size and large distance from earth. But to develop mining technologies for an asteroid, a near-complete information has to be available.
- Low ΔV : This is very crucial for the Spacecraft's journey. Lesser ΔV would directly have a positive impact on the economy of the spacecraft. Besides, the payload and fuel carrying capability depends upon this factor.
- Spin Rate: High spin rate makes it difficult for Landing on an asteroid.
- Size: Adequate size ($>300\text{m}$ diameter) ensures that there is enough ore to be worth the cost and effort.
- Orbital Parameters: Orbital plane, inclination, eccentricity and velocity are some very important parameters crucial in developing the reference trajectory of a spacecraft and as such directly impact the prospection of an asteroid.
- Type: C-Type or Carbonaceous asteroids contain potential volatile minerals which is the primary focus of the mining mission. More details are presented in the subsection below.

1.2.2 | Purpose of Targeting C-Type Asteroids

C-type asteroids are named after the carbonaceous minerals they possess. Many volatile-bearing phases have been discovered in carbonaceous asteroids through studies conducted on its spectral properties and analysis of meteoritic samples. These phases include phyllosilicates, clay and organic compounds which are known to release gas when

heated to sufficient temperatures. Extraction of volatile compounds such as water, carbon dioxide and methane from these bodies make them favourable targets for Space Mining processes. These volatile minerals in space provide us an excellent opportunity to locally produce spacecraft propellant and other life-support gases like water and oxygen. Hydrogen, oxygen, carbon and sulphur compounds may be produced from carbonaceous ore and utilized, either in raw form or processed into more useful end-products.

1.2.3 | Narrowing Down to Particular Asteroids

Our search for asteroid selection for mining purposes initially began with searching and listing down a number of asteroids which fit into our selection criteria. There are a large number of asteroids catalogued, but only a few of them have been studied and analysed to an appreciable extent. For this reason, the focus was shifted to those asteroids which have already been visited by some spacecraft or which were on the radar of space agencies for their past/ongoing/future missions.

1.2.4 | A Comparative Study

After a definite period of going through a particular number of asteroids, 2008 EV5 and Bennu were chosen for a comparative study at the end of which we selected our final prospect asteroid for mining.

1.2.4.1 | Shape and Porosity

BENNU: Bennu has a ‘spinning-top’ shape, more like a diamond-shaped viewing from the poles, with an equatorial ridge. It is a rubble pile asteroid, that is gravitationally bound, unconsolidated fragments with very low bulk tensile strength. Bennu’s shape and surface features imply that the asteroid has some structural rigidity, despite being a rubble pile. The total porosity of Bennu is 50–60% —similar to that of other carbonaceous (C)-group asteroids suggesting a monolithic nature.

2008 EV5: It is an oblate shaped spheroid (muffin-shaped). The most prominent surface feature is a ridge parallel to the asteroid’s equator that is broken by a concavity 150 m in diameter. The concavity is interpreted as an impact crater. The asteroid surface is more likely to be a pebble-rich lag depleted of fines, and as such, the near-surface porosity should be higher and the compaction lower than the asteroid’s bulk compaction and porosity.

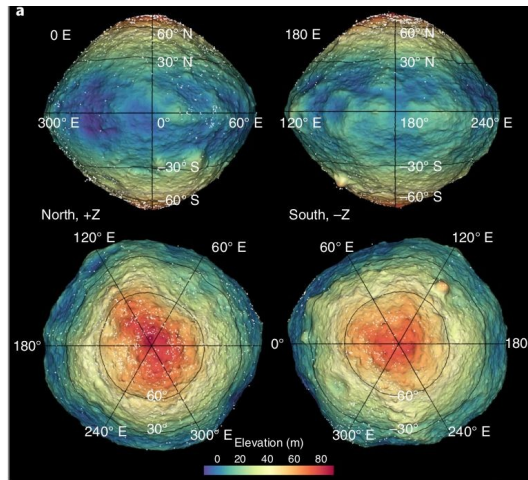


Figure 1.1: Elevation on the asteroid 'Bennu'

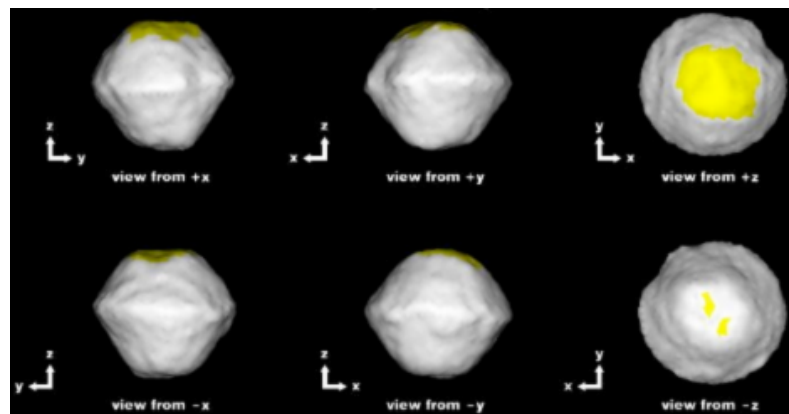


Figure 1.2: The different views of the asteroid '2008 Ev5'

1.2.4.2 | Temperature Distributions

BENNU: Lower values of the thermal inertia imply higher temperatures. The polar regions are cooler than the equator. Less temperature-altered organics are more likely to be found on the south pole rather than on the north pole.

2008 EV5: Results from initial dynamical modelling of 2008 EV5's migration from its most likely origin to its current orbit showing the probability that 2008 EV5's surface exceeded a given temperature and the corresponding perihelion for each surface temperature.

Probability	2%	14%	24%	44%	60%	80%	100%
Surface Temperature	1030K	730K	600K	510K	460K	420K	340K
Perihelion	0.1AU	0.2AU	0.3AU	0.4AU	0.5AU	0.6AU	0.9AU

1.2.4.3 | Surface Features

BENNU: Bennu's surface has equatorial and longitudinal ridges, large boulders, craters, mass-wasting deposits and linear features. The spatial distribution of boulders on the surface of Bennu is not uniform. Size ranges from » 20m to some 10m in Diameter. Several large distinct craters are located on Bennu's equatorial ridge.

2008 EV5: Based on 2008 EV5's radar scattering properties and the highest-resolution images of asteroid surfaces (Eros and Itokawa) from spacecraft, there are likely millions of 10-cm scale cobbles on 2008 EV5. Generally speaking, relatively flat, boulder-populated areas are predicted to occur on 2008 EV5. Boulders on 2008 EV5 could exhibit strength characteristics that fall within the following ranges:

- Shear Strength: 0.1 - 5 MPa
- Compressive Strength: 0.5 - 50 MPa
- Tensile Strength: 0.05 - 3 MPa

1.2.4.4 | Regolith

BENNU: Elevation and slope data of the surface suggest that there would be loose surface materials near the poles than at the equator. There is some evidence that fine-grained material of the centimetre-scale sizes is present on the surface. To Navigate the Spacecraft around Bennu, some factors to know are the Dust Concentration Upper Limit, Dust Mass Upper limit and Dust Production Upper Limit which are 1.5×10^9 particles, 10^6 g and 1g/s respectively.

2008 EV5: The asteroid's surface is notably smooth on decametre scales. Coarse gravel (1 cm or greater) is expected to exist on the surface overlaying fine grained material. The studies on regolith grain size have resulted in the mean-grain size of 6.6mm to 12.5mm radius.

1.2.4.5 | Minerology Composition

BENNU: Bennu's spectra indicate that the surface is consistent with aqueously altered CM chondrites and lesser amounts of CI material is also present. Bennu's surface is volumetrically dominated by phyllosilicates and represents aqueous alteration of the

parent body. There is high Mg/Fe proportions in phyllosilicates. Magnetite is believed to be a product of aqueous alteration and is present in abundances.

2008 EV5: Remote measurements of 2008 EV5 show that it is a carbonaceous (C-type) asteroid that is believed to be water/volatile-rich and may contain significant amounts of organic materials. 2008 EV5 is not a metal-rich asteroid based on its radar-albedo analysis. Spectral observations of 2008 EV5 are consistent with CI carbonaceous chondrite Orgueil.

1.3 | Conclusion

The above comparative study between Bennu and 2008 EV5 provided a deep insight as to which asteroid should be selected for mining purposes. Based on comparative observations, 2008 EV5 proved to be a better prospect as its mineralogy composition shows more potential minerals than Bennu regarding volatile-bearing phases. Also, the surface temperatures of 2008 EV5 are slightly less than Bennu. After reckoning over other comparative aspects, the team decided to choose 2008 EV5 as a final prospect.

1.3.1 | 2008 EV5

As mentioned above, the spectrum of 2008 EV5 is consistent with the CI carbonaceous chondrite Orgueil. We further carried out studies concerning the volatiles or minerals that we could get from mining.

The Orgueil meteorites are one of the most studied meteorite composition since a CI type Orgueil meteorite first fell in southern-western France in 1864. The meteorite was studied and scientists reported the presence of iron sulphides, hydrated silicates, and carbonates. High water and carbon contents were also noticed. A petrographic and transmission electron microscopic study of the Orgueil CI carbonaceous chondrite show that matrix consists of mainly Fe-bearing, Mg-rich serpentine and saponite as well as poorly crystallized Fe-rich material. Below table shows Orgueil simulant mineralogy:

Serpentine and olivine group minerals are major phases present in carbonaceous asteroids and represent opposite ends of the spectrum in terms of volatile production. While serpentine minerals are estimated to produce 12-13 wt.% water from hydroxyl groups present in their crystal structure, a pure olivine mineral is not expected to produce gas under the test conditions

Meteorite Type	Subgroup	Asteroid Type	Major Simulant Minerals	Wt.%
Volatile-rich			Mg-serpentine	48
Carbonaceous	CI	D, P, C	Magnetite	13.5
Chondrites			Vermiculite	9
			Olivine	7
			Pyrite	6.5
			Epsomite	6
			Smectite	5
			Sub-Bituminous Coal	5

1.4 | Challenges

With limited access to information a number of challenges were faced during studying the prospect asteroid, which hinder the development of ideas for mining. Below listed are the problems we faced:

- As for mining purposes it was very difficult to estimate the surface hardness of the asteroid. This was an obstacle in developing the drilling system.
- A major problem was how would the surface micro-gravity affect our lander and other subsystems.
- For extraction of minerals how deep we would have to mine? There was no idea how to counter this problem.
- What would be the composition under surface: rocky, chunks or coarse/fine regolith? This proved to be a major obstacle.
- Some of the environment conditions were very difficult to estimate.

Design Overview

2.1 | Brief Description of the Proposed Lander Design

The below figure is a 3-D Model of the proposed Lander Design. It is a mobile mining robot with 4 legs each of which has a Microspine Anchor attached at its feet. Microspines are very efficient and effective anchoring mechanisms which can be used in unstructured and unknown environments as is explained in the next section. The 3 coring drills for drilling and extraction of water have been fitted at the bottom of the robot symmetrically with respect to its center.

2.2 | Anchoring to the Asteroid: Microspine Anchoring Technology

2.2.1 | Introduction

Till date, successful landing on small bodies has been a rare achievement, performed only by a few Space Agencies like JAXA and ESA during their Hayabusa 2 and Rosetta Mission, respectively. While Rosetta was only able to perform a soft landing on the surface of comet Churyumov-Gerasimenko, Hayabusa 2 was able to both land and collect samples from the surface of asteroid Ryugu. But to perform mining operations, we need more than just landing. Proposed here is a Coring drill + Auger mining technique. Drilling requires a minimum preload force that pushes the drill bit inside the surface, known as Weight-On-Bit (WOB). On the surface of larger celestial bodies like Mars or Moon, the WOB can be reacted by the gravitational force acting on the rover or lander itself. But on the surface of asteroids where the acceleration due to gravity is around

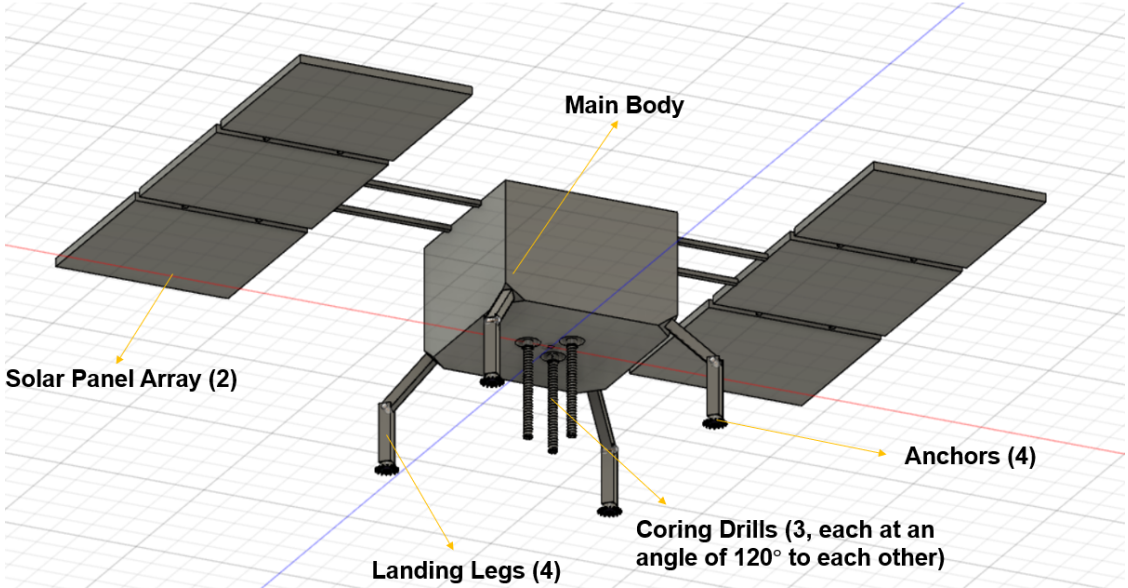


Figure 2.1: Lander Robot 3-D View

10^{-4} m/s², the weight of a spacecraft having a mass of 500 kg is around 0.05 N and the typical value of the WOB can be as high as 100 N. If at all this WOB has to be reacted by the weight of the spacecraft, it should have a mass of 10,00,000 kg which is way beyond the limit of today's rocket launchers. Therefore, establishing strong grip to the surface using some mechanism and using the gripping force as a reaction to the WOB seems inevitable. We propose to employ Microspine anchors to all of the 4 legs of our lander robot, to provide us both the gripping and reaction force (WOB).

Microspines were invented at the Stanford University to provide mobility on rough terrains, Martian lava flows where Rovers can't be employed, rock climbing robots, perching aerial vehicles, etc. cannot be employed. Fundamentally, a microspine consists of simply a sharp hook and a flexible suspension. These tiny sharp steel hooks can latch into small asperities on a rock's surface such as pits, cracks, bulges, grains, slopes, or any other kind of topography that a hook can snag. As the microspine contacts and drags along the surface, the flexible suspension allows the hook to conform to the varying roughness of the surface and stretches as it bears load to allow multiple microspines to engage and share the load. Because each microspine can only support a few N of force before failing, the flexible suspension is required to distribute loads across many microspines within the gripper.

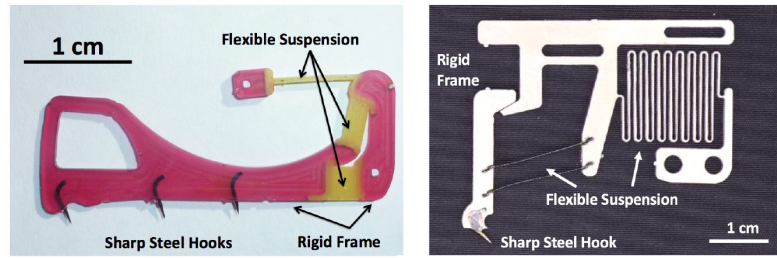


Figure 1: Microspines. Rapid prototype units (left) and space flight capable (right)

Figure 2.2: Microspine Prototypes (Aaron Parness et. al, NASA JPL)

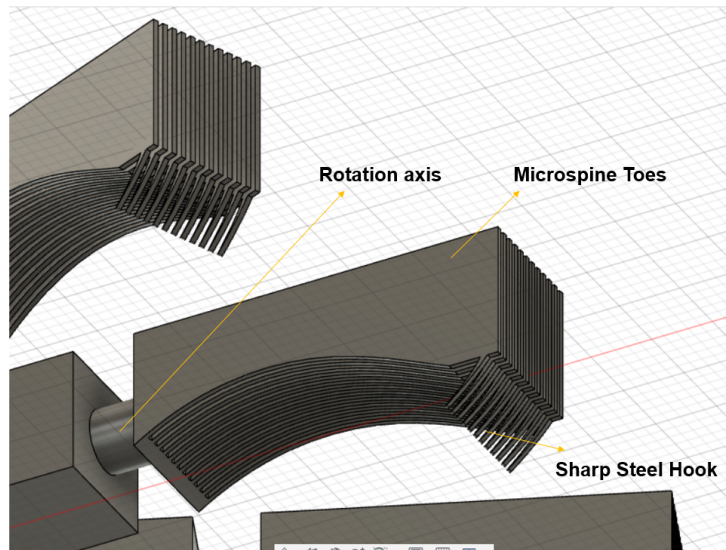


Figure 2.3: A 3-D Model of the Microspines

2.2.2 | Gripper Construction and Working principle

Omnidirectional anchors, proposed by Aaron Parness et. al, NASA JPL, use a radial arrangement of microspines with a centrally located tensioning degree of freedom, as can be seen in Figure 2.4. Regardless of the gravitational orientation, the toes will drag across the rock surface to establish a grip, even in an inverted position. The radial configuration creates a secure anchor that can resist forces in any direction away from the surface. A hierarchical compliance system was developed that contains 16 carriages of microspines that conform to cm-scale roughness. Each carriage contains 12 microspines, which conform to mm-scale roughness and below.

Robotic Ankle: This is a key component to interface the anchor to the lander robot. Its purpose is two-fold: 1) to allow the gripper to conform to the rock so a higher

percentage of microspines attach to the surface, and 2) to neutralize torques that may tend to dislodge the grippers from the surface. The ankle also houses both the engagement and disengagement actuators, which are used for loading and unloading the microspines. A high torque brushed DC motor is used for the engagement actuator while a 2-inch linear actuator for disengagement.

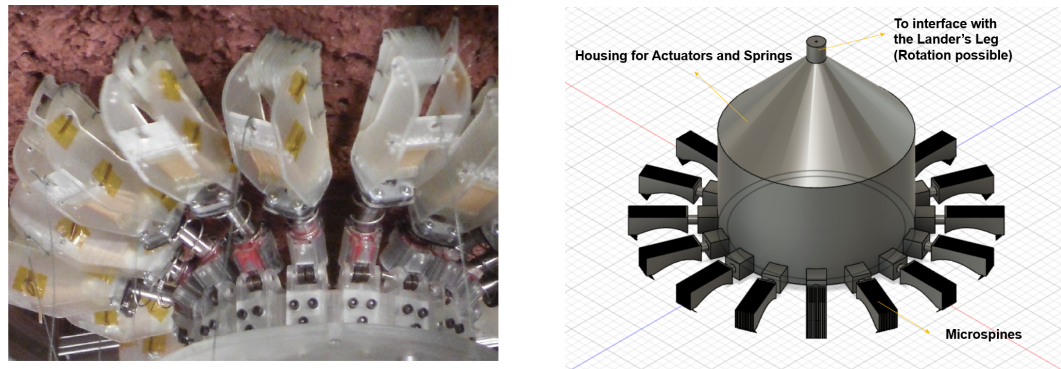


Figure 2.4: Left: Microspine Carriages; Right: Robotic Ankle 3-D Model

2.2.3 | Experimental Results

- The anchor was able to support >160 N tangent, >150 N at 45 degrees and >180 N normal to the surface.
- The anchors were successfully engaged and detached more than 100 times, and were tested to failure of the grip non-destructively.

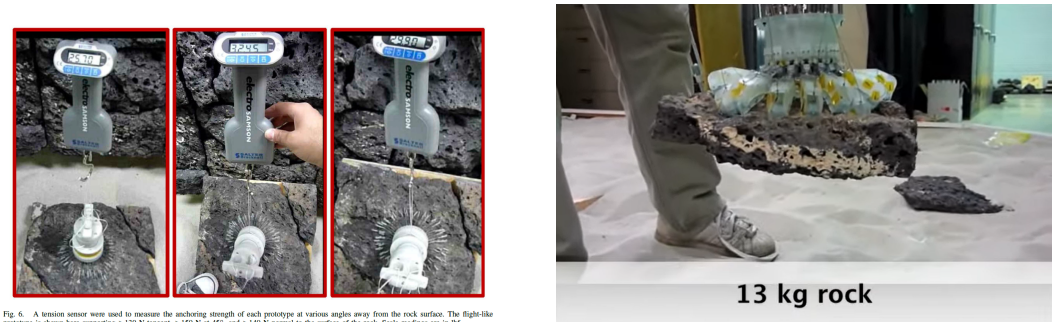


Figure 2.5: Experimental Results

2.3 | Drilling Assembly and Mobility Intuition

At the bottom of the lander, there are three coring drills present at the 3 edges of an equilateral triangle, with the thruster at its centroid. A single drill could have had been chosen, but to cover a larger area in a fixed position and for a larger throughput, more than one drill has to be employed. The power required per drill unit is on an average 225 W for drilling and 800 W for heating but since we have employed 3 drills, the heating time will be 3 times of that required for one drill unit with the same power.

The length of the coring drills is chosen to be 75 to 100 cm while considering the depth at which hydrated minerals can be found inside the surface. To incorporate the long drills, the bottom of the lander is at a height of around 100 cm above the asteroid surface. The legs of the lander are integrated with landing joints (see Figure 2.7) around which rotation is possible. For drilling deeper into the surface, the lander will make use of these joints to lower down to the asteroid surface. The working of landing joints is depicted in Figure 2.7 and 2.8 (Left). The measurement of the drill depth can be done using a LIDAR sensor attached at the bottom of the lander, whose working is shown in Figure 2.8(Right).

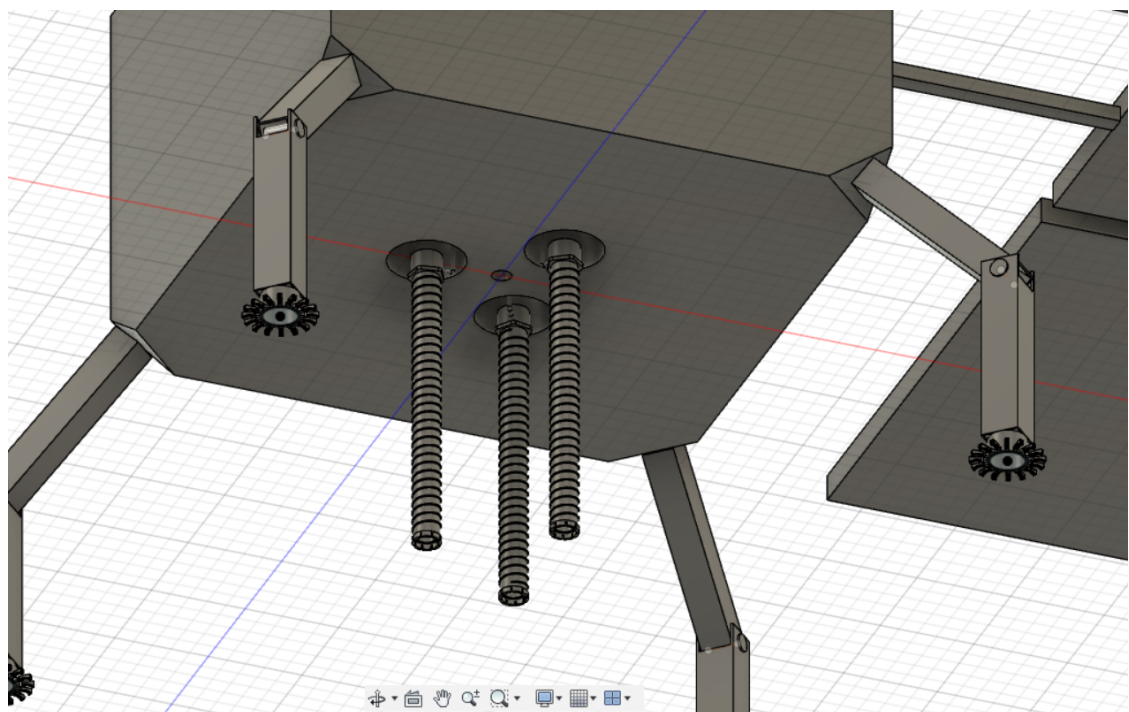


Figure 2.6: Lander Bottom Close-up view

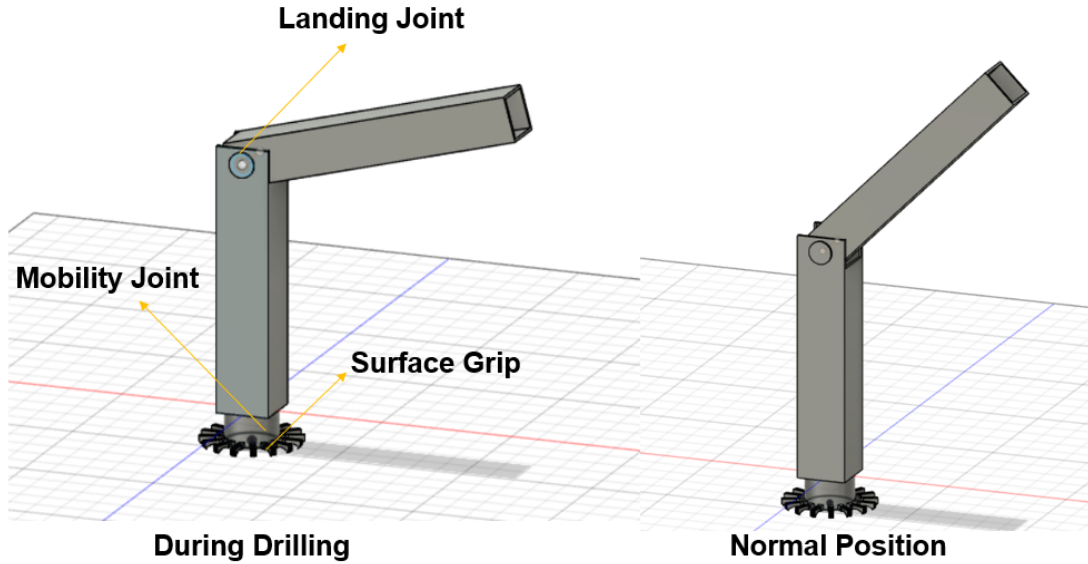


Figure 2.7: Lander Leg position during Normal and Drilling operations

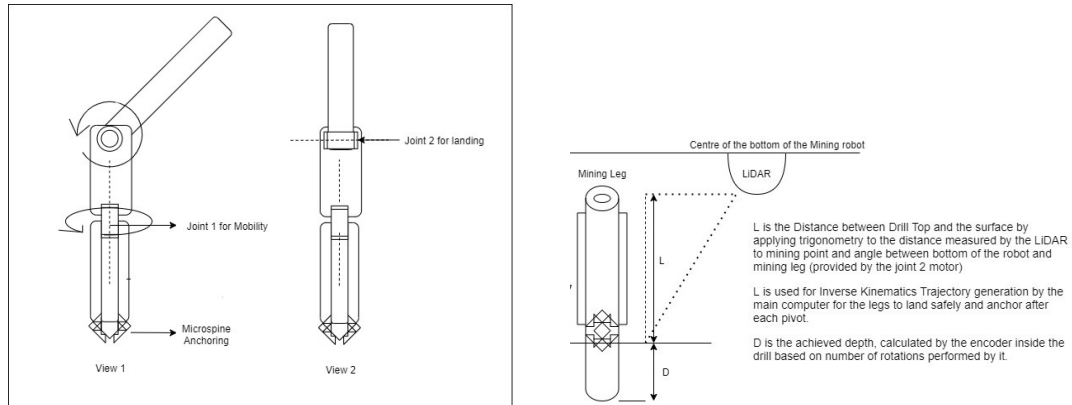


Figure 2.8: Left: Mobility Concept ; Right: Measuring Drill depth

Since there is not much gravity on the surface of asteroids, there are very limited options for a robot to move around on the surface. Also the robot cannot drill at the same place for ever. For the mission to be meaningful, the lander has to cover a large surface area on the asteroid. The Mobility joint, as the name suggests is used for the locomotion of the lander robot. The Robotic ankle, as was shown in the previous section can interface with the lander leg, and neutralize any torques that tend to dislodge the

leg from the surface. There is rotation possible around this ankle, which can be made use of. During mobility, one of the legs depending upon the direction we want to move towards will remain anchored to the surface while all the other 3 will de-anchor using the disengagement actuators. Now the entire robot will rotate about the axis of the anchored leg using a stepper or a servo motor. After the desired position is established, the legs will again be made to anchor to the surface. Since, the actuators do not consume much power, such kind of mobility mechanism is feasible. Also, the actuators will be loaded while there is no power supply, so as to retain the same gripping when power loss occurs during some uncertain event.

Drilling and Extraction

3.1 | Drilling Technique

The Drilling Technique proposed here is suitable for the surface of carbonaceous asteroids. These contain volatile minerals and here we have focused on the extraction of water from the soil. The Drill Assembly is a combination of a shallow Auger and a Corer, where the regolith will be collected and heated in-situ to extract water.

- **Auger:** Its main purpose is to make the drilling operation easier on the rough and widely unknown surface of asteroids. While performing drilling, the shallow auger ensures the side walls of the shaft remain free from coagulation of soil, which may occur due to the micro-gravity environment on asteroid surface. Also, it prevents the soil from collapsing inside the drilling hole. It also helps in tackling sticking of drill inside the hole. Along the inner surface of auger, there is a plastic insulation present, which will prevent the heat from escaping into the surrounding environment, which if not done may cause a faster depletion of water resources.
- **Corer:** It is a cylindrical porous copper container present inside of the auger, which contains embedded micro-printed heaters present all across its inner surface to conduct heat which will be used to provide the necessary temperature needed to cause dehydration of the soil captured. Between the plastic insulation and the outer surface of the Corer, there is space for the volatile to escape into the cold finger, which is depicted in the below figure.

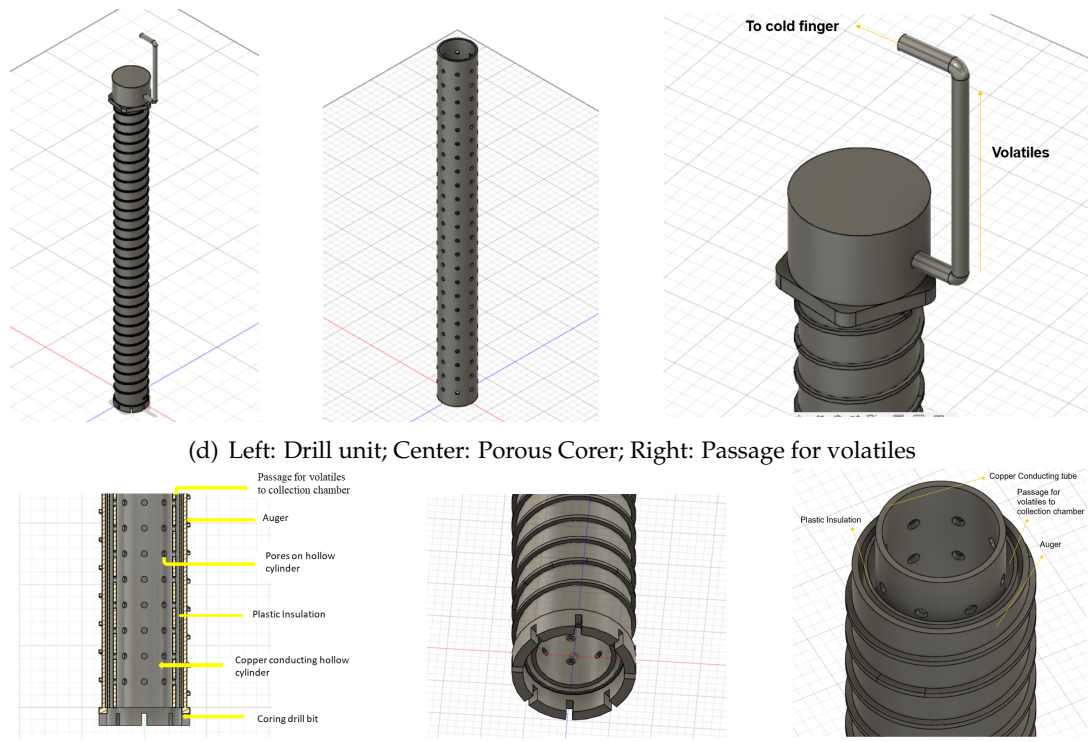


Figure 3.1: Drilling Assembly

3.2 | Heating the soil

The design consists of two walls where the core is captured within the inner wall. The inner wall is perforated (porous) and generates heat which sublimes the volatiles present in the core. The vapours escape through the pores into the cold finger naturally due to the pressure difference (between hot air and cold air). The focus is on generating an efficient heating technique for the inner wall.

3.2.1 | Challenges

- The tube is porous and hollow which rules out many heating options.
- The gap between the inner and outer walls is only 10mm.
- The heating system must be very compact and effective.
- The power requirements must be monitored appropriately.

- The heat generated must be uniformly distributed along the surface area of the wall to get maximum efficiency.
- The weight of the heating system should not be high.

3.2.2 | Technique Proposed

Keeping in mind all of the above challenges, we propose the use of micro-printed heaters.

Micro-printed heaters are basically heating elements which can be embedded throughout the perforated inner wall. By doing so, we can ensure the inner wall is heated uniformly.

The inner wall is made up of metal possibly copper and the membrane can be embedded with micro printed heaters and thermocouples (to sense temperature) These elements do not add any significant weight to the system. Mesoscribe Technologies is one of the leading manufacturers of printed heaters and we believe the same can be incorporated into our design The heaters would be printed throughout the inner wall and the heat is generated when connected to power source. The resistance of each heater can be varied to achieve the required temperature.

ADD FIGURES HERE

3.2.3 | Results

A version of this embedded heaters was used in the testing of PVEx-Corer drilling technique (from which our design is majorly inspired) and was found to deliver good results

Test Results:

Diameter of Outer wall	7.1 cm
Diameter of Inner wall	6 cm
Length of the Drill	75 cm
Heater Power Required	727 W

These numbers are feasible for our design. Specifications (Advantages):

- Printed heaters are compatible with almost all metals (copper, stainless steel, aluminium etc) and many polymers like Kapton, LCP, Tedlar etc
- Can reach temperatures as high as 500 Degree Celsius and in groups can handle heat flux of upto 500 W/sq cm
- Erosion resistant and Damage tolerant (suitable for our mission)

Parameter	Value	Notes
Total Energy per day, kWhr	71	
Drill Energy/day, kWhr	5	
Heat Energy/day, kWhr	66	
Battery Energy Density, kWhr/kg	0.180	
Battery mass assuming 4 charge/discharge cycle per day, kg	100	Required energy: 71/4=18 kWhr
MMRTG Heat Generation, kW	2	MSL-type
MMRTG Heat Generation per 24 hr day, assuming 25% losses	36	
MMRTG Electrical Power Generation, kW	0.1	MSL-type
MMRTG Electrical Energy Generation per 24 hrs, kWhr	2.4	
MMRTG Mass, kg	40	
Number and mass of MMRTGs for all Electrical and Heat per day,	2 80 kg	2x36 kWhr of heat 2x2.4 kWhr of Electrical Energy

Figure 3.2: Overall Performance

- Thermal shock resistant (-200°C to 200°C)
- Previous have been used in certain satellites and launch vehicles

Phase	Reaction	Volatile Evolved	Approximate Temperature of Evolution (°C)
Adsorbed Water	Desorption/Dehydration	H ₂ O	<300
Ferrihydrite	Dehydration/Decomposition	H ₂ O	100-200, 500-600
Mg-Serpentine	Decomposition	H ₂ O	400-600
Saponite	Dehydration/Decomposition	H ₂ O	400-600, 700-800
Gypsum	Dehydration/Decomposition	H ₂ O, SO ₂	<200, 1200
Epsomite	Dehydration/Decomposition	H ₂ O, SO ₂	310, 1100
Ni-Blodite	Dehydration/Decomposition	H ₂ O, SO ₂	260
Tochilinite	Dehydration/Decomposition	H ₂ O, SO ₂	<400, 400-600
Breunnerite	Decomposition	CO ₂	400-650
Dolomite	Decomposition	CO ₂	700
Calcite/Aragonite	Decomposition	CO ₂	890
Sulphur	Oxidation	SO ₂	<200
Sulphides	Oxidation	SO ₂	400-600
Intermolecular Organic Matter (IOM)	Oxidation	H ₂ O, CO ₂ , SO ₂	-

Figure 3.3: Composition and Temperature Required

The above table gives us a rough indications of temperatures at which different volatiles are evolved. The table shown suggests that our heating technique would be good enough to efficiently extract water. However, the temperatures at which volatiles

evolve varies drastically from asteroid to asteroid because it primarily depends on the surroundings. Any substance boils at the temperature at which its vapour pressure equals the surrounding pressure.

Sensors and cameras

4.1 | Main Structure Design

Literature review was applied by the participants in order to retrieve possible architecture designs from previous projects. As it is displayed in the below image, some previous schematic structures provided the general idea of implementing the honeybee approach.

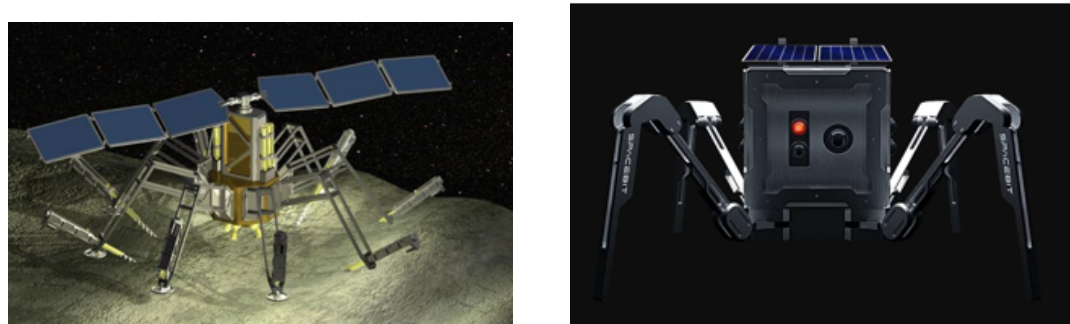


Figure 4.1: Left:8-leg spider robot design ; Right: : Concept Asteroid Water Extractor, designed for reconnaissance and resource collection

There have been some asteroids exploration projects in which deep research has been developed. As a result, engineering prototypes are available. For example Hayabusa project implemented a big spacecraft which transported containers which worked as main physical repositories for mining robots exploration.

In the first Hayabusa Project, ARProbes were used for collecting samples while spiders were used for mining extraction. The original spider is inspired in the traditional 8

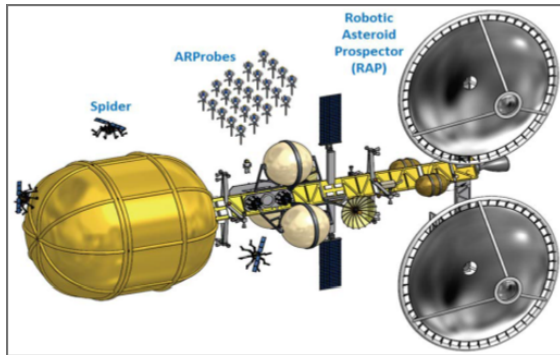


Figure 4.2: Spacecraft Carrying Spatial Station including Spiders and ARProbes (Asteroid Reconnaissance Probes)

legs spider. Even though, other robots with less number of legs have been designed and used depending on designing factors such as energy consumption, required traction strength, working temperature, etc.

As it is displayed in figure 4.1 (right), a 4-leg robot was designed by Robohub intended for the exploration and water extraction.

After considerable applied research, the Vulcans team has worked and analyzed a feasible solution with takes into account the energy and drilling requirements. The design is intended to take most benefits from the honeybee robot design in terms of compactness and functionality.

4.2 | Proposal for Implementation of Sensors and other Electronic Modules

The implementation of sensors is crucial for improving main capabilities from the mining robot. According to the proposed design in figures 3 and 4, two main systems can be implemented in order to take advantage of space in the main design.

4.2.1 | Space Robotics LIDAR System

LIDAR is an active remote sensing system. It means, its going to consume energy for a certain period of time. There are several advantages using this subsystem. One of the main functions is to obtain the range to one or more points on a target spacecraft. LIDAR sensors use light to illuminate the target and measure the time it takes for the emitted signal to return to the sensor.

The target consists of the main asteroid which might have an approximate dimension from 300 m to 1 Km radio size. Once the spacecraft is near the asteroid, the navigation control system will be managed so the distance between the target and the satellite is near 300 meters.

Hayabusa-2 is the second asteroid mission of Japan and LIDAR is one of five instruments onboard that measures altitudes of the spacecraft from a surface of the asteroid, by taking a time of flight of laser pulse. LIDAR is a part of attitude and orbit control subsystem and is designed for navigation of the spacecraft, in particular, during touchdown phase. LIDAR data are scientifically important for analysis of the shape, mass, and surface properties of the asteroid.

The laser mechanism, called YAG, has a wavelength of 1.064 micro-meters. The size of this equipment is 240 x 240 x 230 mm, and weighs 3.7 kg. Shape and mass of the target asteroid is determined to elucidate the nature and history of accretion and destruction of rubble pile body. The model is developed basically from ONC images and LIDAR range data. LIDAR range data determines its length scale. Mass is also essential for geodetic study of C-type asteroid.

4.2.2 | Spacecraft Positioning

The strategy is to let the spacecraft descend toward the target asteroid from 25 km to 30 m altitude without orbital maneuvers, and let the spacecraft ascend freely as well. The number of times the spacecraft descends or ascends, depends on the fuel left in the spacecraft. The advantage of this design comes by the measurement of both transmitting and receiving powers which might be useful for qualitative analysis.

The above table contains original information from Hayabusa 2 LIDAR. The altitude range is high enough so the spacecraft can be used for medium to big size targets. The resolution is high enough so measurements are high precise to determine an accurate position of the spacecraft. The 127 mm telescope diameter ensures that debris and other kinds of particles are clearly identified. The power consumption is 18.5 W which does not represent a high investment in terms of resources.

LIDAR can provide a time resolution of less than 3.33 ns corresponding to 0.5-m range resolution. Telemetry and command are transferred between LIDAR and the ground station via the Attitude and Orbit Control System (AOCS). The range data passed to AOCS are used to keep the spacecraft in a safe distance from the asteroid or control touchdown approach.

Finally, it is important to consider that the laser altimeter LIDAR requires the presence of some other sensors which might be useful for prospective analysis As a result,

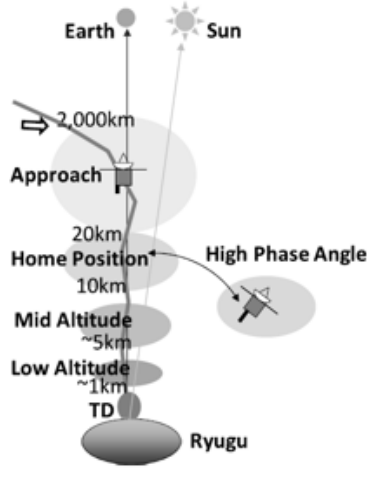


Figure 4.3: Spacecraft positioning taking into account the use of LIDAR

Parameter	Value
Altitude range	30 m ~ 25 km or longer
Range resolution	0.5 m
Range accuracy (1 s.d.)	± 1 m or less (at 30-m altitude) ± 5.5 m or less (at 25-km altitude)
Telescope Diameter	127 mm
Pulse width	10 nsec or less
Receiver detector	Si-APD
Power consumption	18.5 W (w/o survival heater)

Figure 4.4: Main Parameters Specification in LIDAR

the full scientific observation equipment contains an optical navigation camera, the laser altimeter LIDAR, the near-infrared spectrometer NIRS3 and the thermal infrared camera TIR as displayed in figure 4.5.

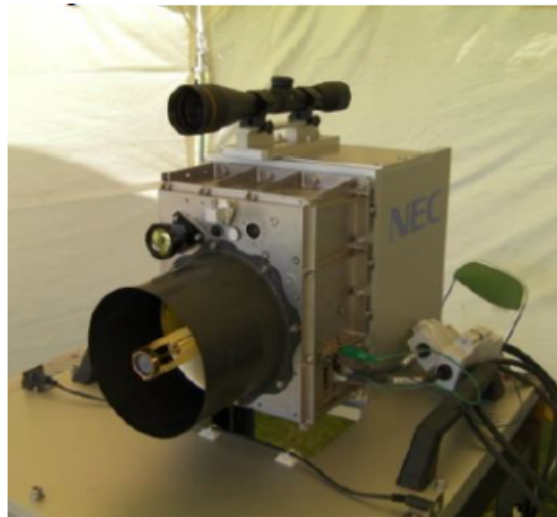


Figure 4.5: Laser Altimeter LIDAR

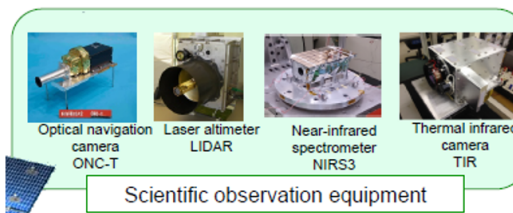


Figure 4.6: Scientific observation equipment from Hayabusa 2

4.2.3 | Scientific Objectives and Conclusions from Laser Altimeter (LIDAR) Light Detection And Ranging

LIDAR is a navigation sensor used for approach and landing at a target, and a scientific observation device used to measure shape, gravity, surface characteristics, and for dust observations. In that way, important information is retrieved as the asteroid form, mass, porosity, and deviation. Asteroid surface roughness and dust floating phenomena is also retrieved.

The scientific objectives are focused in terrain and gravity field observations of the target asteroid, observations of albedo distribution at various surface point and observations of dust floating around the asteroid.

4.3 | Optical Navigation Camera

The optical navigation camera is an optimal solution implemented in Hayabusa-2. It consists of one telescopic camera (T) and two wide-angle cameras (W1 and W2). The ONC-T is a telescopic camera with seven band-pass filters in the visible and near-infrared range. In table 2, layout parameters from the 3 ONCs are listed.

Designs of ONC	ONC-T	ONC-W1	ONC-W2
Effective aperture (designed value)	15.1mm	1.08mm	1.08mm
Focal length (measured value)	120.50 ± 0.01 mm for wide-filter	10.22mm	10.34mm
Field of view	6.27° (Nadir view)	69.71° (Nadir view)	68.89° (Slanted ~30° from nadir)
Effective F# (designed value)	9.05	9.6	9.6
Color filters	7 color bandpass filters (ul: 0.40 μm, b: 0.48 μm, v: 0.55 μm, Na: 0.59 μm, w: 0.70 μm, x: 0.86 μm, p: 0.95 μm) and 1 clear filter (wide).	Clear filter	Clear filter

Figure 4.7: Layout Parameters from ONCs

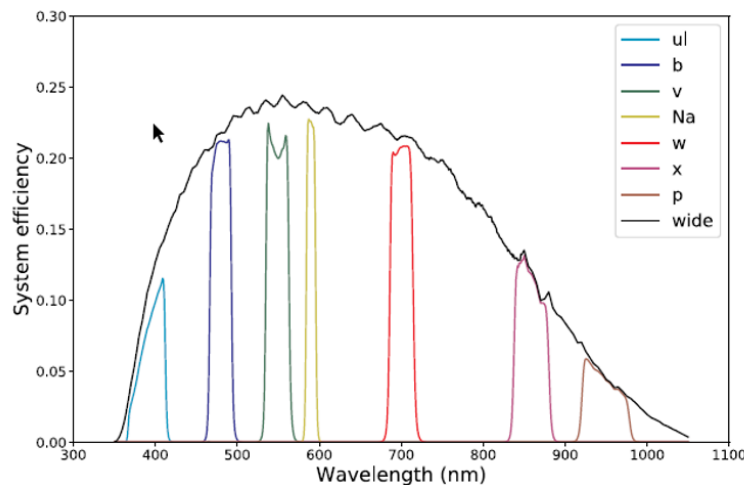


Figure 4.8: System efficiency of ONC-T bandpass photometric system

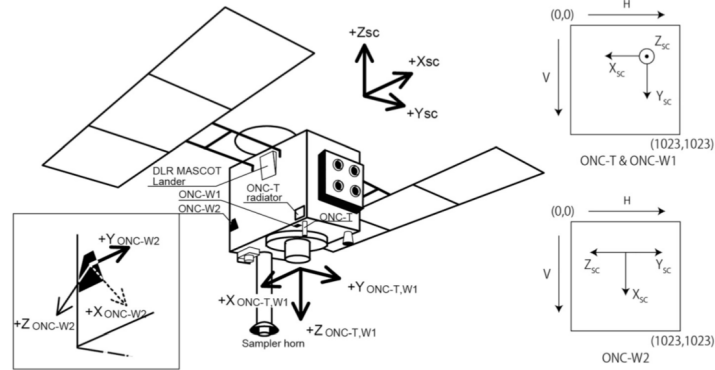


Figure 4.9: The spacecraft coordinate system and the image coordinate system

ONC-T Specification		
Optics	Focal length	120 mm
	F#	8
	Effective aperture	$\varnothing 15$ mm
	Field of view	$6.35^\circ \times 6.35^\circ$
	Pixel resolution	22 arcsec/pixel
	Depth of field	100 m ~ infinity
	Transmittance of	30%
	ND filter	
Filter wheel	Band pass filter	#1:ul 0.39 um, #2:wide*, #3:v 0.55 um, #4:w 0.70 um, #5:x 0.86 um, #6:Na 0.59 um, #7:p 0.95 um, #8:b 0.48 um
	Filter wheel driving rate	9.6°/s (4.69 s/filter)
CCD	CCD	e2v CCD47-20 (AIMO)
	Pixel format	1024(H) pixel - 1024(V) pixel
	Pixel pitch	13 lm - 13 nm
Electronics	Dynamic range	10 bit
	A/D bit length	

Figure 4.10: ONC-T Specifications

The performance of these sensors is high and valuable information might be retrieved from them. In figure 4.9, the original position of these sensors is referred.

4.4 | Sensors used in the mining process

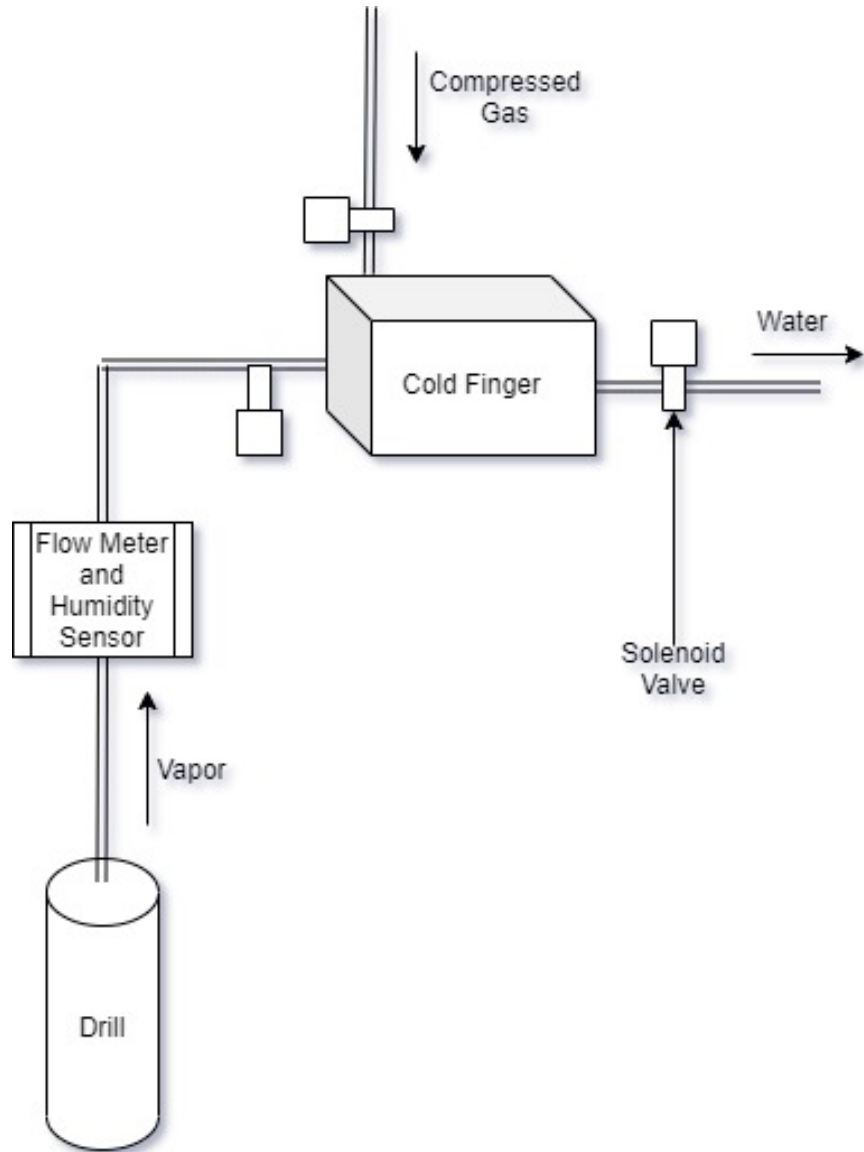


Figure 4.11: Extraction Process

The above figure represents the process of extraction of water vapor and the mechanisms involved. The vapor flows from the drill through the flowmeter and humidity sensor suite and into the cold chamber. There are three valves for the cold finger. After the cold finger is full, the input valve closes, and the other two open, with the compressed gas pushing out the water into the storage tank.

The sensors incorporated into our design which are essential for many processes are listed below.

- **Flowmeter** - A transducer to output the amount of vapor passed based on calibration data, there are many types like Turbine flowmeters, Ultrasonic flow meters etc. for this application. Turbine Flowmeters are advantageous when the rate of flow is low but may face problems with steam condensation and affects the accuracy.

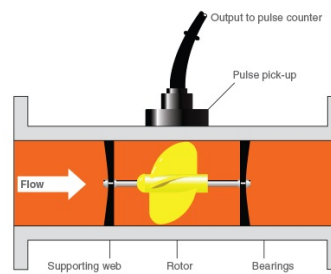


Figure 4.12: Turbine flow meter

- **Humidity Sensor** – A sensor used to detect the presence and amount of humidity in the vapor, used as a fool proof detection of water vapor presence and to detect the point of exhaustion of water in the respective mining cavity. **Temperature Sensor Modules** – To detect system temperature and surface temperature and the main computer will consider these to control the thermal subsystem.
- **In drill Composition Sensor** – These are a set of embedded sensors inside a drill and are used to find the composition of the rocks/regolith and at different depths. Referenced from the Honeybee Robotics Design

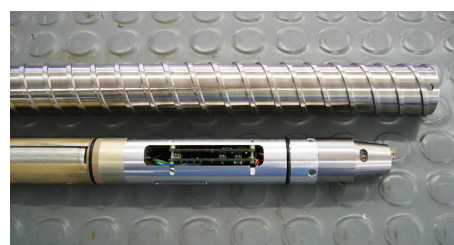


Figure 4.13: In drill Composition Sensor

- Inertial Measurement Units – IMUs are position and orientation measuring sensors consisting of a set of gyroscopes and accelerometers to accurately measure different dynamic parameters in a spacecraft. These are used in our mining robot to keep a track of its position on the asteroid with reference to the main host orbiter/lander as it moves around mining in different places. This combined with 3D Mapping of the asteroid surface by prospection drones using LiDAR, works as the Positioning system on the asteroid. This can help the robot to move to a target place and avoid redundant movements to already exhausted mining areas. It provides data to the computer for controlling of the thrusters especially in case of unexpected toppling of the robot.

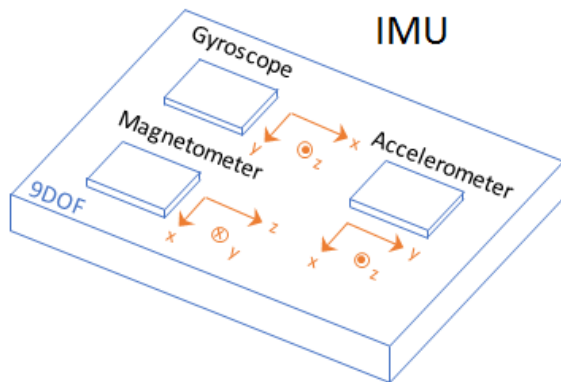


Figure 4.14: Inertial Measurement Unit

Power Subsystem

5.1 | Introduction

Power subsystem is responsible for delivering the power to all other subsystems based on their requirements. The team is responsible for the design of power source, storage, condition and control unit. In all the designs and calculations we have considered mainly 3 asteroids for comparison, Bennu, Ryugu and 2008 EV5(Our prospect asteroid).

The major components of the Power subsystem are shown in Figure 5.1. Energy from the sun in the form of radiation is the only energy source available in the space environment, all other alternative primary sources have to be carried by the spacecraft for its mission, such as Radioisotope Thermoelectric Generator (RTG), Fuel cell and battery. Source along with secondary storage units such as Batteries and power distribution, control and protection units form the Power subsystem of any space based mission.

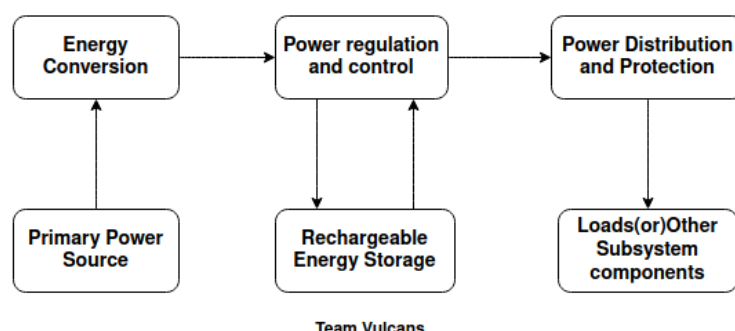


Figure 5.1: Broad Overview of Power subsystem.

5.2 | Power Source Design

Selection of suitable power source depends on various parameters such as:

- Power Budget
- Mission Location
- Mission Type
- Duration
- Cost Budget
- Technology readiness level

Now, in our case we are not working on a power critical mission, so a negligible shortage of power for a small-time does not lead to mission failure. But as our mission objective involves various processes such as drilling, heating and cooling, the power requirement is higher when compared to missions involving sample collections. As our prospect asteroid, which is 2008 EV5, has the worst case distance from the sun as 1.038 A.U, for which we get satisfactory Solar Irradiance of 1281 W/m^2 . Hence the usage of Solar power as the primary power source will be a feasible option. Since the power requirement is quite high we thought of including the RTG and Solar in a blended fashion. But our team calculated and found that usage of solar alone will be sufficient to provide the required peak power. So we went ahead with the design considering solar as our primary power source. Figure 5.2 shows the initial architecture considered, whereas Figure 5.3 shows the finalized power subsystem architecture with few modifications.

And also, in the Mars rover missions like Curiosity and Perseverance, RTGs were used as the primary power source to supply continuous power and whenever the peak power requirement exceeds the power that can be delivered through RTG, batteries were used to meet the power demands. But most of the available designs of RTG can deliver only power up to 120-130 W (One design BES-5 can deliver a power of around 3kW but the power to mass ratio is very low as it weighs almost a 1000Kg and this increases the Launch Cost as the ΔV of our asteroid is not very less), As the TRL of new designs were not up to the standards and also there are solar panels designed and tested for missions with kilowatts of power requirements, we moved to solar power as a viable and feasible option.

In the design process, the first step is to list down the overall power requirements, where we collect data from all the subsystem components. The data includes peak

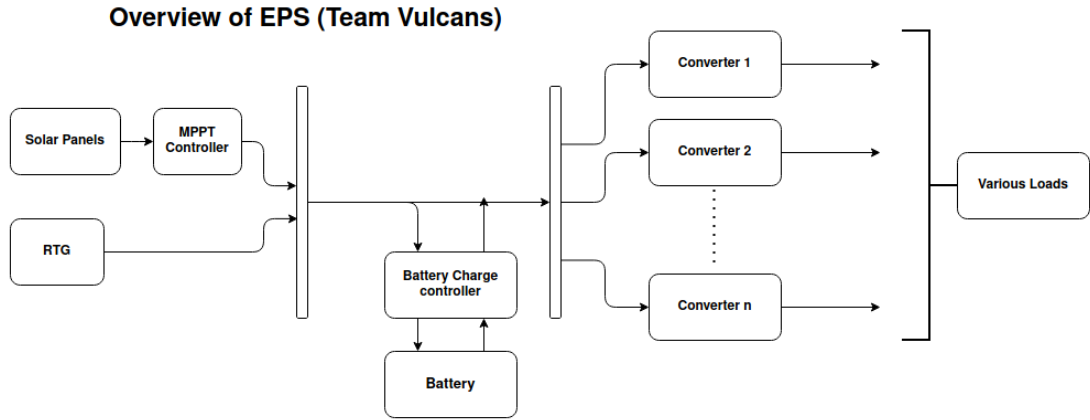


Figure 5.2: Initial Architecture

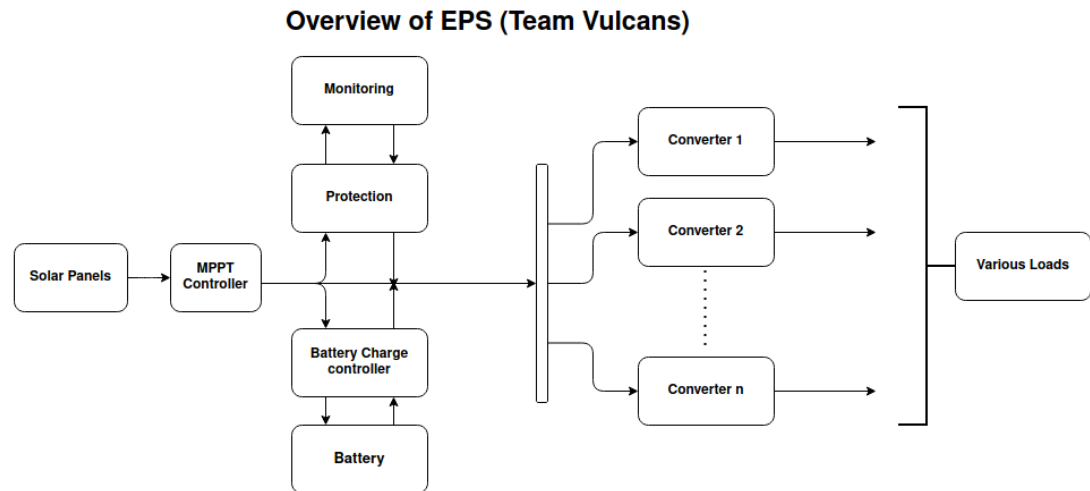


Figure 5.3: Finalized Architecture

power requirement, average power requirement and duty ratio. But in our case, as we were not designing end to end system, peak power demand alone is sufficient for the design. The design of solar panels is such that it should provide peak power requirement at the end of life, which is the worst-case scenario as all the subsystems working simultaneously is a very unlikely and rare event. The requirements of different subsystems are shown in Table 5.1.

The total peak power requirement is 2.394 kW, from the architecture we can see that

Subsystems	Peak Power(W)
Drilling	675
Auger Heating	800
Cooling Chamber	150
Actuators for Microspine	120
Thermal Subsystem	200
TTC, ADCS and OBC	50
Margin(20%)	399
TOTAL	2394

Table 5.1: Peak power requirements of all subsystem components

the path of power flow takes place through various electronic and electrical components and not directly from the source to load, hence we need to account for the loss of power along the circuit, which we call as the EPS (Electrical Power Subsystem) efficiency. Typical Converter Efficiency is around 90-95%, so we took the worst case scenario and calculated the power backwards. As 2.394kW of power is required after the converter stage,

$$\text{Power Required Before Converter Stage} = \frac{\text{Power Required After Converter Stage}}{\text{Converter Efficiency}} \quad (5.1)$$

We get Power required before the converter stage to be 2.66 kW, On the similar lines other circuit elements account for approximately another 3-5% of the power, which gives us the power required at the output of solar to be equal to 2.8 kW. For the design considerations we need the approximate efficiency of the solar cell, so at the current technology we can get 30% efficient solar cells which are typically made of Ga-As, and usage of multi-junction solar cells are preferred over a single junction as they have higher theoretical and practical efficiency over a long time.

The amount of solar array area facing normal to the sun is known as effective solar array area, and power output of solar panels depends on the tilt angle, which means reduced effective area, which is cosine functions of declination angle and off-set angle.

$$P = I * V * i * \text{Cos}(\delta) * \text{Cos}(\psi) \quad (5.2)$$

Where,

P = Power generated

V= Bus Voltage

I = Solar array Generated Current

i = Intensity Factor

$$\delta = \text{Sun declination angle}$$

$$\psi = \text{Sun off set angle}$$

We calculated the effective array area as part of our design. To get the idea of how much array area is required, we did a comparative analysis of array sizes on various places like Earth, Mars, Bennu, Ryugu, and our prospect asteroid 2008 EV5. For Earth, Inherent degradation factor and ageing is assumed to be 2%. For Mars, as the atmosphere is thin, the GaAs cells degrade 2-3% per year due to radiation on Mars and 2% due to wind loading dust.

Property	Earth	Mars
Irradiance	1360 W/m ²	588 W/m ²
Solar cell efficiency at BOL	30%	30%
Solar cell output at BOL	408 W/m ²	176 W/m ²
Solar cell efficiency at EOL	28%	25%
Solar cell output at EOL	380 W/m ²	147 W/m ²
Total power requirement	2800 W	2800 W
Effective solar array area required	7.368m ²	19.048 m ²

Table 5.3 Array design on Earth and Mars

As we have selected NEA(near earth asteroid) , and they are in between earth and mars we can infer from the above result, that the effective array area required for those asteroids will be in between 7.368 m^2 and 19.048 m^2 .

- For Bennu,which is at 1.313 A.U from sun as on 07-09-2020, worst case will be at aphelion which is 1.3558 A.U
- For Ryugu,which is at 1.243 A.U from sun as on 07-09-2020,worst case will be at aphelion which is 1.416 A.U
- For 2008 EV5,which is at 0.943 A.U from sun as on 07-09-2020,worst case will be at aphelion which is 1.038 A.U

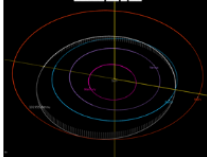
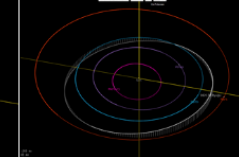
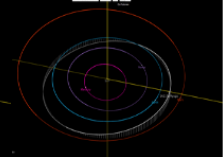
Property	Bennu	Ryugu	2008 EV5
Orbit Diagram (Origin-Sun White-Asteroid Orbit Blue-Earth Orbit Red-Mars Orbit)			
Irradiance	751.17 W/m ²	688.63 W/m ²	1281 W/m ²
Solar cell efficiency at BOL	30%	30%	30%
Solar cell output at BOL	225.35 W/m ²	206.65 W/m ²	384.3 W/m ²
Solar cell efficiency at EOL	26%	26%	26%
Solar cell output at EOL	195.30 W/m ²	179.09 W/m ²	333.06 W/m ²
Total power requirement	2800 W	2800 W	2800 W
Effective solar array area required	14.337 m ²	15.635 m ²	8.407 m ²

Table 5.4.Array Design on asteroids Bennu,Ryugu and 2008 EV5.

5.3 | Battery Design

Solar arrays cannot supply power during an eclipse or night in an asteroid and certain peak load demands. The battery is designed to supply an uninterrupted power during the night duration of the asteroid and also at certain peak demands. The battery charges during the day through the solar arrays and discharges to the various loads during the eclipse period.

As the battery is to be recharged during the sun-lit time, the battery to be designed is considered to be a secondary battery. To calculate the battery capacity required, the team has calculated the eclipse time of the asteroid and the estimated eclipse load requirements.

Assuming the asteroid to be a roughly spherical body, the eclipse duration of any spherical asteroid is given by,

$$\text{Eclipse Duration} = \frac{\text{Rotational Period}}{2} \quad (5.3)$$

Asteroid Bennu, Ryugu and 2008 EV5 have rotational periods of 4.297 hours, 7.627

hours and 3.725 hours respectively. Thus the eclipse time is calculated to be 2.1485 hours, 3.1835 hours and 1.8625 hours respectively for these asteroids.

The battery has to supply the power demands during the eclipse. Some subsystems do not work during the eclipse to reduce the load. Table 4 shows the individual subsystem load during the eclipse duration of the asteroid.

Subsystems	Normal Load(W)	Eclipse Load(W)
Drilling	675	675
Auger Heating	800	400
Cooling Chamber	150	150
Actuators for Microspine	120	120
Thermal Subsystem	200	200
TTC, ADCS and OBC	50	15
Margin(20%)	399	365
TOTAL	2394	1925

Table 5.2: Eclipse Load Data

During eclipse, it is assumed that the heating operation does not take place to its fullest potential. There will not be telemetry to earth and the on-board computer reduces its operating capability to reduce the power demand. Considering all these factors, the eclipse load is estimated to be 1925W. After considering 90% efficiency of converters we get the peak power to be delivered by the battery designed.

Battery bus voltage is to be determined for the calculation of ampere hour rating of battery. The factors that influence selection of bus voltage for the battery are:

- Power Budget
- Space environment and space plasma.
- Paschen minimum breakdown voltage between bare conductors
- Availability of components, such as semiconductor devices, power distribution and protection devices, tantalum capacitors, etc.

It is found for a mass optimized design of battery,

$$\begin{aligned}
 \text{Optimum bus voltage} &= 0.025 * \text{Normal Load Power} \\
 &= 0.025 * 2394 \\
 &= 59.85V
 \end{aligned} \tag{5.4}$$

As 59.85V is not a standard voltage level, we choose the standard voltage level of 50V for the battery design. The mission duration for all the asteroids is assumed to be 600days, i.e 14400 hours.

5.3.1 | Trade-off between choosing Ni-MH and Li-ion battery

Ni-MH batteries are some of the traditional heritage batteries used in space missions. The Li-ion batteries are the relatively new and rapidly developing type of battery. Due to its advantages over Ni-MH batteries, Li-ion batteries are gaining popularity. Li-ion batteries have higher power to weight ratio. Li-ion batteries do not have memory effects as in the case of Ni-MH batteries. But the only disadvantage of the Li-ion battery is its lower charge-discharge cycle leading to lower durability. We have chosen either of the batteries where the mission requirements favour the battery properties.

5.3.2 | Battery calculation

Ni-MH battery is preferred for asteroids Ryugu, Bennu, 2008 EV5 as the cycle-discharge cycle of the required battery is to be as high as 750 cycles, 1300 cycles and 1500 cycles respectively.

The figure 5.4 shows the steps followed to design the battery for the robotic mission in the asteroid Ryugu, Bennu, 2008 EV5.

As calculated and also shown in Table 5.3, the battery capacity required for the robotic lander in the asteroids Ryugu, Bennu and 2008 EV5 are 19.332 kWh, 10.892 kWh and 9.442 kWh respectively.

5.4 | Conclusion

The Power source design is a crucial part in any space-based mission. Our findings suggest that for a robotic mission in future, the solar as power source is feasible for a near earth asteroid missions. The order of solar array area calculated and its performance are already tested in past space missions, thus establishing reliability on robot's power source. The ratings of the conceptual battery designed is slightly higher. As large scale drilling operation for mining has not been carried out till date in space and thus battery would require rigorous testing and development.

Step	Considerations	Ryugu	Bennu	2008 EV5
Energy Storage requirements	Mission length	14400 h	14400 h	14400 h
	Primary or Secondary battery	Secondary Battery		
	Eclipse Length	3.8135 h	2.1485 h	1.8625 h
	Bus Voltage	50V		
	Depth of Discharge	40%		
	Charge-Discharge cycle limit	~754 cycles	1342 cycles	~1546 cycles
Type of Battery	Secondary Battery	Ni - MH Battery	Ni - MH Battery	Ni - MH Battery
Size of battery	No. of Batteries	N=1 (for total capacity calculations)		
$\text{BATTERY CAPACITY} = \frac{\text{ECLIPSE LOAD} * \text{ECLIPSE DURATION}}{\text{DEPTH OF DISCHARGE} * \text{NO. OF BATTERIES} * \text{EFFICIENCY}}$				
Battery Capacity		19.332 kWh	10.892 kWh	9.442 kWh
$\text{Ampere-hour Rating (A-h)} = \frac{\text{Battery Capacity}}{\text{Bus Voltage}}$				
Ampere - Hour Rating		386.64 A-h	217.84 A-h	188.84 A-h

Table 5.3: Steps to design battery for mission to asteroid Ryugu,Bennu and 2008 EV5

Thermal Control System Analysis and Design

The main objective of the Thermal Control System of a spacecraft is to keep all the components within acceptable temperature range during the different mission phases. This can be achieved by-

- Protecting the components from overheating from the external heat sources (Solar flux, Albedo, IR radiation, Solar flares etc.) by shielding, removal of excessive heat by radiators, louvres, heat pipes etc.
- Prevent freezing temperatures due to exposure to external heat sink (deep space) by heat absorption from external sources, heat retention from internal heat dissipators.

The thermal analysis of Vulcan is carried out only for the mining phase of the mission.

6.1 | Environment

The mission environment is characterized as follows.

- Long mission duration – 2years.
- Extreme thermal conditions in the absence of an atmosphere.
- Landing on a celestial body.
- Icy and dusty conditions are expected.

Temperature requirements of components on board:

6.2 | Preliminary Thermal Analysis

Preliminary Thermal Analysis was carried out on the Vulcan to estimate the Temperature variations the space craft will be subjected to due to the following external heat sources, heat sinks and the internal heat sources.

1. Solar Irradiance
2. Albedo of the asteroid 2008 EV-5
3. InfraRed Radiation being emitted from the asteroid
4. Electric Loads in the interior of the spacecraft
5. Deep Space

6.3 | Model

1. Asteroid: The following assumptions were made.
 - a) The asteroid is a sphere.
 - b) The asteroid is in instantaneous thermal equilibrium.
 - c) The surface temperature is uniform throughout.
 - d) The surface is macroscopically smooth.
2. Vulcan:
 - a) The space craft is a perfect sphere with radius $r = 2\text{m}$.
 - b) Due to the large distance between the sun and spacecraft, the illuminated area at any given point of time can be assumed to be circular disc with the same radius.
 - c) For electrical components without any moving parts, their power consumption is assumed as the heat dissipation.
 - d) For electric motors used in drilling operations, the heat losses are assumed to be 35%.
 - e) The total power consumption of Heater is assumed to be the heat dissipation.
 - f) The entire spacecraft is exposed to deep space temperature $T_a = 2.7\text{K}$.
 - g) The spacecraft is in steady-state.

	Operating		Non-operating		Power Consumption(W)	Heat Dissipated(W)
	Temperature (K)		Temperature (K)			
	Min.	Max.	Min.	Max.		
Battery Charging/Discharging	273/253	323/348	253	333	4900	(0.3*4900) = 1470
TTC, ADCS and OBC	233	358	208	398	50	50
LIDAR, Telescope/Altimeter Subsystem	273	323	273	323	18.5	18.5
Drilling	280	600	200	280	675	(0.35*675) = 236.25
Auger Heating	-	-	-	-	800	800
Cooling Chamber	-	-	-	-	150	150

Table 6.1: Temperature requirements and Heat dissipation of components on board

$$\text{Total Heat dissipation} = 1725.75\text{W}$$

Asteroid InfraRed Radiation

The InfraRed radiation being emitted by the asteroid is a function of its surface temperature.

$$q_{IR} = \sigma * \epsilon * T^4 \quad (6.1)$$

Where,

$\sigma = 5.670373108$ is the Stefan-Boltzmann Constant.

$\epsilon = 0.9$ is the emissivity

$T = 400\text{K}$ is the surface temperature of the asteroid

$$q_{IR} = 3.3*10^{-3} \text{ W/m}^2$$

6.4 | Thermal Analysis

The spacecraft was evaluated for hot case and cold case temperature for a varying value of Absorptivity and Emissivity using MATLAB code (can be found in Appendix A). The following plots were obtained.

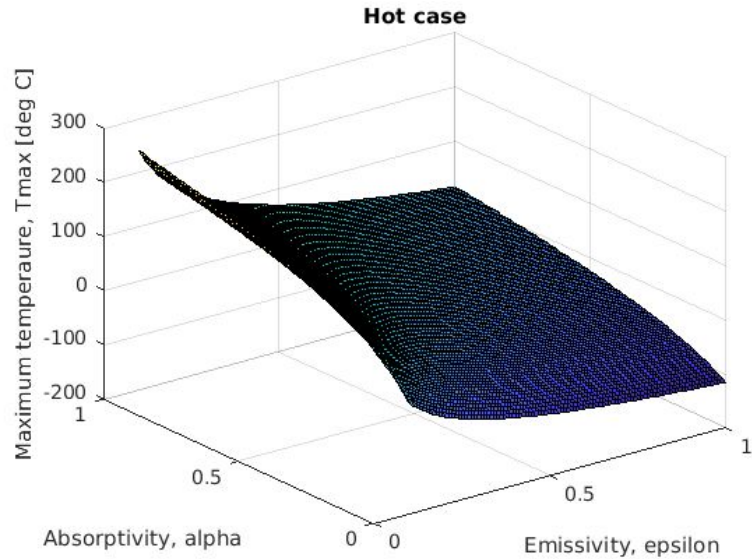


Figure 6.1: Figure 6.1: Hot Case Temperature variation

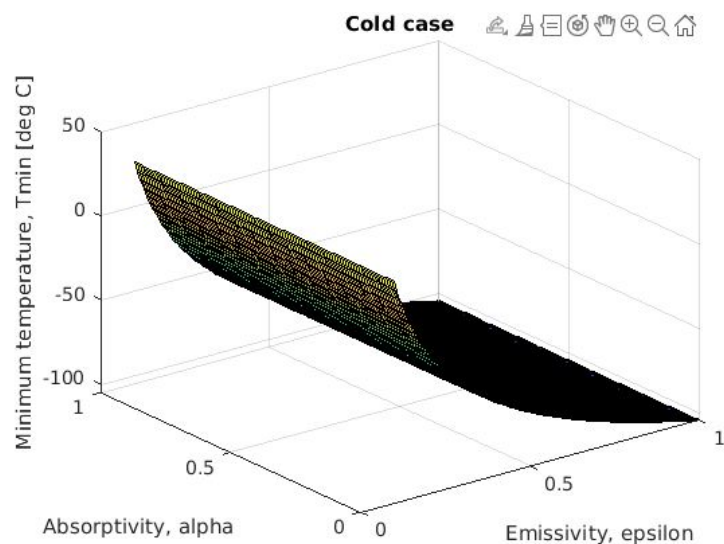


Figure 6.2: Figure 6.2: Cold Case Temperature variation

Since most of the components operate in the temperature range of 0-40 degree Celsius, the hot case was analyzed for temperature in that range (Code can be found in Appendix A).

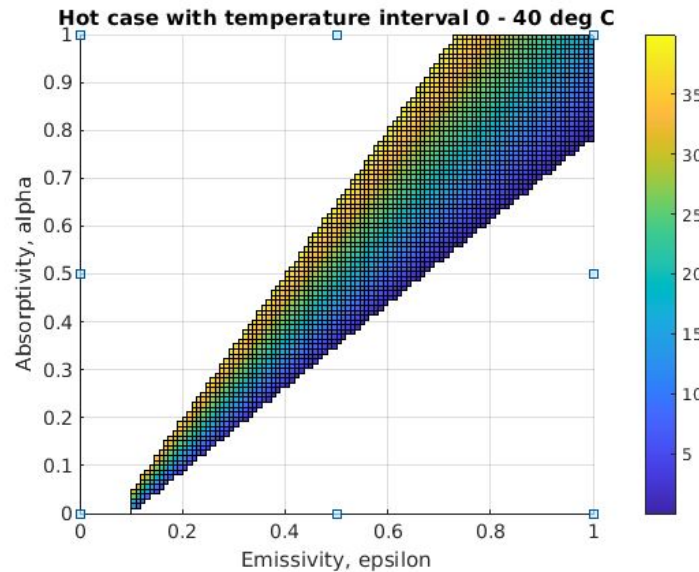


Figure 6.3: Figure 6.3: (0-40) degree Celsius Temperature range

For an operating hot case temperature of about 20 degree celsius, the emissivity and absorptivity were found to be approximately 0.7 and 0.6 respectively. Using these values, the Maximum and Minimum temperatures were found to be 8.97 degree celsius and -88.89 degree celsius respectively.

To estimate the rate of temperature decrease during the eclipse period, the above Maximum and Minimum temperatures were used as the upper and lower limit and the asteroid eclipse period was approximated to be ($223.5/2 = 111.75$ minutes), half of the rotation period.

It was found that the lowest temperature experienced during the eclipse period was about -77 degree Celsius. The asteroid exits the eclipse phase before the spacecraft can reach the minimum temperature of -88.89 degree Celsius. However, the -77 degree Celsius is still below the operating and non-operating minimum temperature of all the components. Hence, a Thermal Control system is needed to keep the components warm during eclipse period.

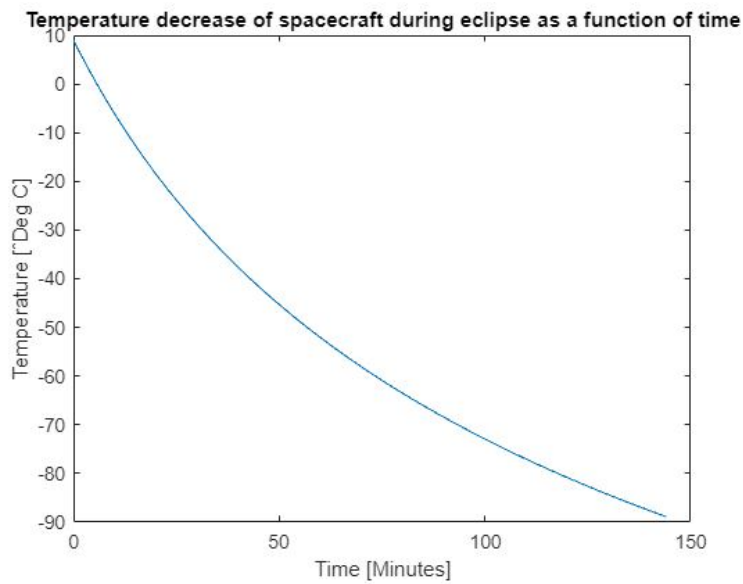


Figure 6.4: Temperature decrease during eclipse period

6.5 | Thermal Control System

Passive thermal control uses no energy and requires no monitoring, whereas active thermal control systems require energy to operate and need monitoring.

A Multi-Layer Insulation (MLI) with low emissivity, suitable thickness and layers can be wrapped around the space craft to prevent the heat loss to the external heat sink. Flexible Patch Heaters can be mounted on critical components to keep them within safe operating temperatures. Thermal control system can be quantitatively modeled using thermal simulation software like Thermal Desktop, Sinda, Siemens NX etc.

Future Scope - Water Electrolysis Propulsion

7.1 | Introduction

Electrolysis of water is a process of decomposing liquid water into gaseous hydrogen and oxygen on the application of electric potential. The propellant tank contains both inert water and the H_2 and O_2 gases in equilibrium. These gases can be passed into the collection chamber, ignited and the resulting high-pressure gases can be expanded in the nozzle to produce thrust on-demand. The energy conversion occurs in the following fashion:

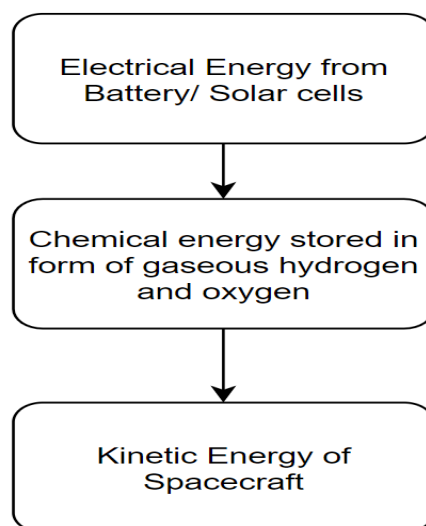


Figure 7.1:

7.2 | Features

- It consists of no active mechanisms, just a flame arrestor between the propellant tank and the combustion chamber and a check valve between the combustion chamber and the nozzle.
- When the gas pressure in the combustion chamber reaches around 10 atm ignition can take place on-demand.
- Working conditions: Liquid water can be stored at low pressures.
- Specific Impulse (ISP) (ratio of generated thrust to the mass of fuel consumed): Water Electrolysis propulsion can provide an ISP of around 300 s and can reach up to 450 s ideally.
- Relative Impulse Density (RID): It is the ratio of the product of Specific Impulse and density of propellant to that of the product of Specific Impulse and Density of Nitrogen cold gas thruster. For Water Electrolysis Propulsion, this value is around 15-20.
- Specific power of 4.5 kW/N at 80% efficiency.
- ΔV as high as 500 m/s can be achieved.
- Water Electrolysis is by itself capable of performing small impulsive maneuvers, thus can be employed in place of a secondary chemical propulsion system.
- Property of Passive Spin Stabilization : Centrifugation process is used to separate the water from electrolyzed gases. The sloshing of water on the walls of the propellant tank during impulsive maneuvers dissipates the Vibrations, thus stabilizing the spin.

7.3 | Advantages over other Propulsion Techniques

Ion propulsion is a very common mode of propulsion especially for deep space missions. It provides a comparatively lower ΔV than Water Electrolysis although it has a Specific Impulse value around 8-10 times greater than Water Electrolysis Propulsion. Also, Xenon and Iodine which are used as in Ion Propulsion are heavy elements.

Other Advantages:

- Water can be used as a Heat sink, Radiation shield and Vibration dampener fluid.

Feature	Water Electrolysis Propulsion	Ion Propulsion
Pressure required for storage	Very low	140 atm (very high)
Specific Power	4.5 kW/N at 80% Efficiency	23 kW/N continuous
Specific Impulse	300 – 450 s	3000 s
ΔV	500 m/s	300 m/s
Relative Impulse Density	15-23	350

Table 7.1:

- Storing liquid propellants like H_2 , CH_4 or O_2 for long durations is a very big challenge. A solution to this problem is using inert water just as in Water Electrolysis Propulsion. Also, water which is abundant on C-type asteroids and small moons, water can be produced IN-SITU using the mining technique proposed and can be used for travelling to other asteroids or even Sample return to Earth.

7.4 | WINE - The World is not Enough

It is an Autonomous Robotic Lander Distribution system proposed by HoneyBee Robotics, for extracting volatiles from the surface of asteroids; produce water in-situ and hop onto other near asteroids after gathering the necessary ΔV .

The water extracted is purified; collected in ice traps; heated and expanded through the nozzle to produce thrust. This kind of propulsion system provides a Specific Impulse of 160 s and a Relative Impulse Density of 8-10, which is very low as compared to Water Electrolysis.

With a propellant load of 3 kg, it can achieve a ΔV of 560 m/s, but Water Electrolysis Propulsion can provide up to 1050 m/s to 1574 m/s, which is 2-3 times greater.

7.5 | Conclusion

Ion propulsion provides impressive Specific Impulse, but has a demerit in the form of larger mass and pressure requirements.

LH_2/LOX appear to be a very attractive option due to its already proven capability but does not provide enough ΔV and Specific Impulse.

Water Electrolysis Propulsion has not been employed yet and is a new area to explore. Theoretical results have given a sense of its capability and will be interesting to study something from scratch.

A.1 |

```

1 % Preliminary Thermal Analysis - Sphere
2 % Preliminary thermal analysis for the spacecraft Lander
3 % Vulcans-SSERD
4 % Jayaprakash B Shivakumar
5 % 09-05-2020
6
7 %%
8 clear
9 clc
10 %%%%% Constants %%%%
11 H = 0; % [m] Orbit altitude - Lander on the surface of asteroid
12 R = 370; % [m] Asteroid mean radius
13 Gs = 1281; % [w/m^2] Solar flux at the asteroid orbit around the sun
14 sigma = 5.670373E-8; % Stefan-Boltzmann constant
15 qIR = [3.3e-3 3.3e-3]; % [Hot value, cold value]
16 Qw = 1725; % [w] Electric energy dissipation
17 eps = 0.7;
18 alpha = 0.6;
19 a = 0.13; % Albedo effect, Hot value,
20
21 A = 4.*pi.*(2.^2); % [m^2]
22 Aabsorbed = pi.*(2.^2); % [m^2]
23
24 %%%% Calculations %%%%
25
26 gamma = asin(R/(R+H));
27
28 F = (1/4 - (((2*(H/R) + (H/R).^2).^0.5)/(4*(1+(H/R)))) ...
29     + (cos(gamma)/8)*(1/(1+(H/R))).^2);
30

```

```

31
32 % Source: http://www.thermalradiation.net/calc/sectionc/C-140.html
33
34 GIR = qIR./(((R+H)/R).^2); % Intensity drops as 1/r^2
35 Gr = a.*Gs.*F;
36
37 Qsolar = alpha.*Gs.*Aabsorbed; % Heat from the Sun
38
39 QIR = eps.*GIR(1).*Aabsorbed;% Heat radiated from Earth seen by the
      spacecraft
40
41 Qalbedo = alpha.*Gr.*A;% Heat from the Sun reflected on the Earth (Albedo)
42
43 Qabsorbed = Qsolar + QIR + Qalbedo;% Total heat from the space environment
      on the spacecraft
44
45 disp('Maximum temperature in Degrees Celcius')
46 Tmax = ((Qabsorbed + Qw)./(sigma.*eps.*A)).^(1/4) - 273.15 % OBS: Celcius
47
48 disp('Minimum temperature in Degrees Celcius')
49 % In eclipse, only radiation from the Earth and internal heating will
      contribute
50 Tmin = ((eps.*GIR(2).*Aabsorbed + Qw)./(sigma.*eps.*A*(3/4))).^(1/4) -
      273.15 % OBS: Celcius ONLY (3/4) of the sphere see 'deep space' and
      radiates to it!

```

Listing A.1: Code 1: Preliminary Thermal Analysis

A.2 |

```

1 %%%%%% alpha - epsilon - temperature 3D plot %%%%%%
2 clear
3 clc
4
5 %%%% Constants %%%
6 H = 0; % [m] Orbit altitude Lander on the surface of the Asteroid
7 R = 370; % [m] Asteroid mean radius
8 Gs = 1281; % [W/m^2] Solar flux at the asteroid orbit around the sun of
      about x AU
9 sigma = 5.670373E-8; % Stefan-Boltzmann constant
10 qIR = [3.3e-3 3.3e-3]; %[258 216]; % [Hot value, cold value]
11 Qw = 1725; % [W] Electric energy dissipation
12 eps = linspace(0.1,1);
13 alpha = linspace(0,1);
14 a = 0.13; % Albedo effect, Hot value

```

```

15 A = 4.*pi.*2.^2; % [m^2]
16 Aabsorbed = pi.*2.^2; % [m^2]
17
18
19
20 %%%%%% Calculations %%%%%%
21 gamma = asin(R/(R+H));
22 F = (1/4 - ((2*(H/R) + (H/R).^2).^0.5)/(4*(1+(H/R)))) + ...
23 (cos(gamma)/8)*(1/(1+(H/R))).^2;
24
25 % Source: http://www.thermalradiation.net/calc/sectionc/C-140.html
26 GIR = qIR./(((R+H)/R).^2); % Intensity drops as 1/r^2
27 Gr = a.*Gs.*F;
28 for i = 1:length(alpha)
29     Qsolar = alpha(i).*Gs.*Aabsorbed; % Heat from the Sun seen by the
      spacecraft
30
31     QIR = eps.*GIR(1).*Aabsorbed; % Heat radiated from Earth seen by the
      spacecraft
32
33     Qalbedo = alpha(i).*Gr.*A; % Heat from the Sun reflected on the Earth
      (Albedo)
34
35     Qabsorbed = Qsolar + QIR + Qalbedo; % Total heat from the space
      environment on the spacecraft
36
37     Tmax(i,:) = ((Qabsorbed + Qw)./(sigma.*eps.*A)).^(1/4) - 273.15;
38
39     Tmin(i,:) = ((eps.*GIR(2).*Aabsorbed + Qw)./(sigma.*eps.*A*(3/4)))
      .^(1/4) - 273.15; % OBS: Celcius
40
41 end
42
43 for i = 1:length(alpha)
44     for j = 1:length(eps)
45         if ((Tmax(i,j) > 0) && (Tmax(i,j) < 40))
46
47             Tmaxreq(i,j) = Tmax(i,j);
48
49         else
50             Tmaxreq(i,j) = NaN;
51         end
52     end
53 end
54

```

```

55 figure(1)
56 surf(eps, alpha, Tmax)
57 title('Hot case')
58 xlabel('Emissivity, epsilon')
59 ylabel('Absorptivity, alpha')
60 zlabel('Maximum temperaure, Tmax [deg C]')
61
62 figure(2)
63 surf(eps, alpha, Tmin)
64 title('Cold case')
65 xlabel('Emissivity, epsilon')
66 ylabel('Absorptivity, alpha')
67 zlabel('Minimum temperature, Tmin [deg C]')
68
69 figure(3)
70 surf(eps, alpha, Tmaxreq)
71 title('Hot case with temperature interval 0 - 40 deg C')
72 xlabel('Emissivity, epsilon')
73 ylabel('Absorptivity, alpha')
74 zlabel('Maximum temperaure, Tmax [deg C]')

```

Listing A.2: Absorptivity Emissivity and Temperature Study

A.3 |

```

1
2 %%
3 %%%% Solve the integral numerically %%%%
4 clear
5 clc
6 H = 0; % [m] Orbit altitude, Lander on the surface of the Asteroid
7 R = 370; % [m] Asteroid mean radius
8 Gs = 1281; % [w/m^2] Solar flux at the asteroid orbit around the sun of
              about x AU
9 sigma = 5.670373E-8; % Stefan-Boltzmann constant
10 qIR = 3.3e-3; %%[Hot value, cold value]
11 Qw = 1725; % [w] Electric energy dissipation
12 eps = 0.7;
13 a = 0.13; % Albedo effect, Hot value
14 Area = 4.*pi.*2.^2; % [m^2]
15 Aabsorbed = pi.*2.^2; % [m^2]
16 Ta = 2.7; % Ambient temperature of 2.7 Kelvin
17 m = 500; % Mass of spacecraft, 500kg
18 C = 897;
19

```

```

20 QIR = eps.*qIR.*Aabsorbed;
21 A = (Area.*eps.*sigma)./(m.*C);
22 B = (QIR + Area.*eps.*sigma.*Ta.^4)./(m.*C);
23
24 Tstart = 273.15 + 8.97;
25 Tend = 273.15 - 88.89;
26
27 T = linspace(Tstart, Tend); %Tend:0.001:Tstart;%T = T(end:-1:1);
28 f = 1./(B - A.*T.^4);
29
30 for i = 1:length(T)
31     Tint = linspace(Tstart, T(i));
32     f = 1./(B - A.*Tint.^4);
33     t(i) = trapz(Tint,f);
34 end
35
36 T = T - 273.15;
37
38 figure(3)
39 plot(t./60,T)
40 title('Temperature decrease of spacecraft during eclipse as a function of
        time')
41 xlabel('Time [Minutes]')
42 ylabel('Temperature [ Deg C]')
43 hold on

```

Listing A.3: Eclipse Temperature drop

References

- [1] V Alí-Lagoa, L Lionni, M Delbo, B Gundlach, J Blum, and J Licandro. Thermophysical properties of near-earth asteroid (341843) 2008 ev5 from wise data. *Astronomy & Astrophysics*, 561:A45, 2014.
- [2] Andreas Berggren. Design of thermal control system for the spacecraft mist, 2015.
- [3] Katelyn Elizabeth Boushon. Thermal analysis and control of small satellites in low earth orbit. 2018.
- [4] Charles D Brown. *Elements of spacecraft design*. American Institute of Aeronautics and Astronautics, 2002.
- [5] Pablo Calla, Dan Fries, and Chris Welch. Asteroid mining with small spacecraft and its economic feasibility. *arXiv preprint arXiv:1808.05099*, 2018.
- [6] Kyle P Doyle and Mason A Peck. Water electrolysis propulsion as a case study in resource-based spacecraft architecture (february 2020). *IEEE Aerospace and Electronic Systems Magazine*, 34(9):4–19, 2019.
- [7] Ken R Erickson. Optimal architecture for an asteroid mining mission: System components and project execution. In *AIP Conference Proceedings*, volume 880, pages 896–903. American Institute of Physics, 2007.
- [8] David G Gilmore. Space thermal control handbook–volume i: Fundamental technologies. 2002.
- [9] Alan W Harris and Johan SV Lagerros. Asteroids in the thermal infrared. *Asteroids III*, 205, 2002.

- [10] Vide Hellgren. Asteroid mining: a review of methods and aspects. *Student thesis series INES*, 2016.
- [11] G Hirzinger. Space robotics. *IFAC Proceedings Volumes*, 27(14):695–714, 1994.
- [12] Nozomi Hitomi and Daniel Selva. Incorporating expert knowledge into evolutionary algorithms with operators and constraints to design satellite systems. *Applied Soft Computing*, 66:330–345, 2018.
- [13] Hao Jiang, Elliot W Hawkes, Christine Fuller, Matthew A Estrada, Srinivasan A Suresh, Neil Abcouwer, Amy K Han, Shiquan Wang, Christopher J Ploch, Aaron Parness, et al. A robotic device using gecko-inspired adhesives can grasp and manipulate large objects in microgravity. *Science Robotics*, 2(7), 2017.
- [14] Robert Karam. *Satellite thermal control for systems engineers*. American Institute of Aeronautics and Astronautics, 1998.
- [15] VLADIMIR KONYUKH. Robotics for mining. *Mineral Resources Engineering*, 11(01):73–88, 2002.
- [16] Aaron Parness. Anchoring foot mechanisms for sampling and mobility in microgravity. In *2011 IEEE International Conference on Robotics and Automation*, pages 6596–6599. IEEE, 2011.
- [17] Aaron Parness, Thomas Evans, William Raff, Jonathan King, Kalind Carpenter, Andrew Willig, Jesse Grimes-York, Andrew Berg, Edward Fouad, and Nicholas Wiltsie. Maturing microspine grippers for space applications through test campaigns. In *AIAA SPACE and Astronautics Forum and Exposition*, page 5311, 2017.
- [18] Aaron Parness, Matthew Frost, Nitish Thatte, and Jonathan P King. Gravity-independent mobility and drilling on natural rock using microspines. In *2012 IEEE International Conference on Robotics and Automation*, pages 3437–3442. IEEE, 2012.
- [19] Mukund R Patel. *Spacecraft power systems*. CRC press, 2004.
- [20] Baiju Payyappilly and M Sankaran. Design framework of a configurable electrical power system for lunar rover. In *2017 4th International Conference on Power, Control & Embedded Systems (ICPCES)*, pages 1–6. IEEE, 2017.
- [21] Petr Pravec and Alan W Harris. Fast and slow rotation of asteroids. *Icarus*, 148(1):12–20, 2000.

- [22] Tomasz Rybus, T Barciński, J Lisowski, J Nicolau-Kukliński, K Seweryn, M Ciesielska, K Grassmann, J Grygorczuk, M Karczewski, M Kowalski, et al. New planar air-bearing microgravity simulator for verification of space robotics numerical simulations and control algorithms. In *proceedings of 12th Symposium on Advanced Space Technologies in Robotics and Automation*, 2013.
- [23] BR Uma, M Sankaran, and Suresh E Puthanveettil. Multijunction solar cell performance in mars orbiter mission (mom) conditions. In *E3S Web of Conferences*, volume 16, page 04001. EDP Sciences, 2017.
- [24] Mark Yim, Kimon Roufas, David Duff, Ying Zhang, Craig Eldershaw, and Sam Homans. Modular reconfigurable robots in space applications. *Autonomous Robots*, 14(2-3):225–237, 2003.
- [25] Kris Zacny, Marc M Cohen, Warren W James, and Brent Hilscher. *Asteroid Mining*.
- [26] Kris Zacny, Marc M Cohen, Warren W James, and Brent Hilscher. Asteroid mining. In *AIAA Space 2013 Conference and Exposition*, page 5304, 2013.
- [27] Kris Zacny, K Luczek, A Paz, and M Hedlund. Planetary volatiles extractor (pvex) for in situ resource utilization (isru). In *15th Biennial Conference on Engineering, Science Construction, and Operations in Challenging Environments*, 2016.